2.5. Electron microscopy

Transfected 293T cells were fixed with 2% glutaraldehyde in 0.1 M cacodylate buffer for 1 h, postfixed with 1% OsO4 for 30 min and stained with 1% uranyl acetate for 2 h. After dehydration in a graded series of ethanol (from 80% to 100%), the cells were embedded in Quetol 812. Ultrathin sections (100 nm) were made on MT5000 Ultra-Microtome (Sorvall) and then examined under an H-7100 electron microscope (HITACHI).

2.6. Immunofluorescence microscopy

Transfected 293T cells were fixed with 1% formaldehyde solution, permeabilized with 0.1% NP40, and then stained with the NOR-1 antibody or the α-c-myc polyclonal antibody followed by FITC- or RITC- conjugated secondary antibodies, respectively.

3. Results

3.1. PPxY motif but not PTAP sequence plays an important role in HTLV-1 budding

To determine which motif is critical for HTLV-1 budding, 293T cells were transfected with 0.5 μg of the wild-type or mutated Gag expression vectors, and the VLPs in the culture medium were quantified. To check the expression levels of the Gag protein, we performed western blot analyses, using NOR-1. The VLP release of ΔPPP and ΔPPP–PTAP mutants was severely inhibited, whereas the ΔPTAP mutant showed slight reduction to approximately 65% of the wild type (Fig. 1C). The expression levels of ΔPPP and ΔPTAP Gag proteins were similar to that of wild-type Gag, although ΔPPP–PTAP mutant looked relatively unstable (Fig. 1D). We also constructed the Gag expression vector encoding a mutant form of the PPPY L domain by replacing Pro-118 of pGag wild type with Ala. VLP release of the APPY mutant was reduced similarly to that of ΔPPP mutant (data not shown). In addition, we examined these experiments at different times (24 and 36 h after transfection). Enough the intensity of ELISA signal or western band could not be obtained at 24 h. The experiments at 36 h showed similar results to those of our 48-h experiments (data not shown). Thus, our data suggest that while the PPPY sequence is required for HTLV-1 budding, the PTAP sequence does not play an important role in this process. In addition, we suppose that the reduction in VLP release by the ΔPTAP mutant may be caused by the conformational effect on the PPPY sequence, because only two amino acids exist between the PPPY and PTAP sequences (see Fig. 1A). However, we cannot exclude the possibility that the PTAP sequence has a weak role in HTLV-1 budding. Supporting these observations is the recent report by Le Blanc et al. [26] that the PPPY motif is required for HTLV-1 virion production.

3.2. Morphological examination of ΔPPP and ΔPTAP mutant budding

To further confirm that the PPxY motif but not the PTAP sequence is required for HTLV-1 budding, we examined the budding process of the wild-type and mutated Gag by electron microscopy. Fig. 2A shows the VLPs of wild-type Gag. The VLPs do not have an electron dense core, due to the absence of a viral protease, similar to that of BLV Gag reported previously [23]. In cells transfected with the ΔPPP mutant, no VLPs could be detected in extracellular medium, and the electron-dense thickenings were found on the plasma membrane (Fig. 2C), similar to PPPY point mutants that Le Blanc et al. reported [26]. In cells transfected with the ΔPTAP mutant, VLPs could be detected in extracellular medium, and pinching off formations of Gag were found on the plasma membrane (Fig. 2D,E). These findings indicated that the ΔPTAP mutant of HTLV-1 Gag shows no significant defect in the late assembly step. Thus, these results support the PTAP sequence of HTLV-1 Gag not playing an important role in the HTLV-1 Gag budding process. In contrast, the PPPY motif is suggested to be required for an earlier step of the HTLV-1 budding process than the pinching-off step.

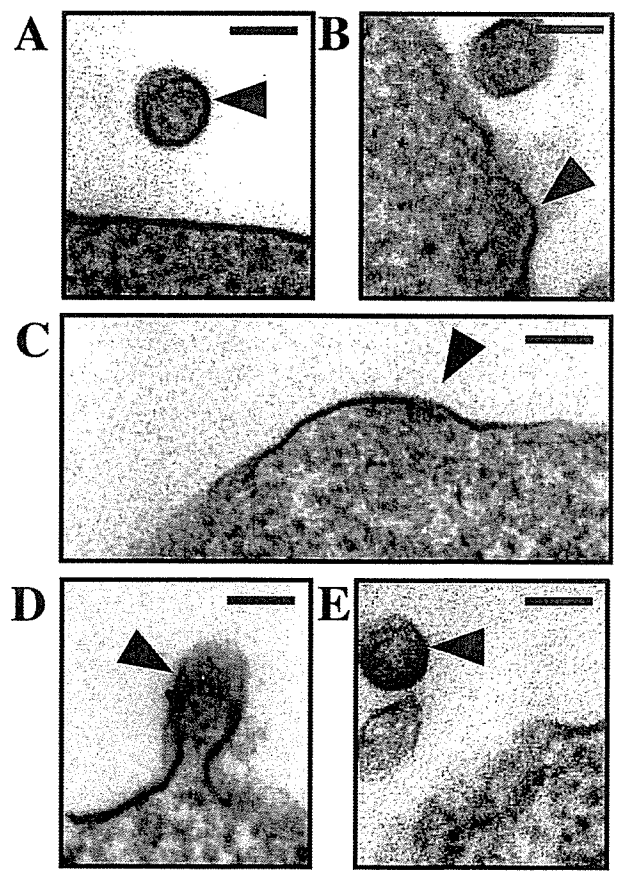

Fig. 2. Electron micrographs of 293T cells transfected with the wild-type or deletion mutant Gag expression vector. (A, B) wild-type Gag. (C) ΔPPP Gag. (D, E) ΔPTAP Gag. Bar: 100 nm.

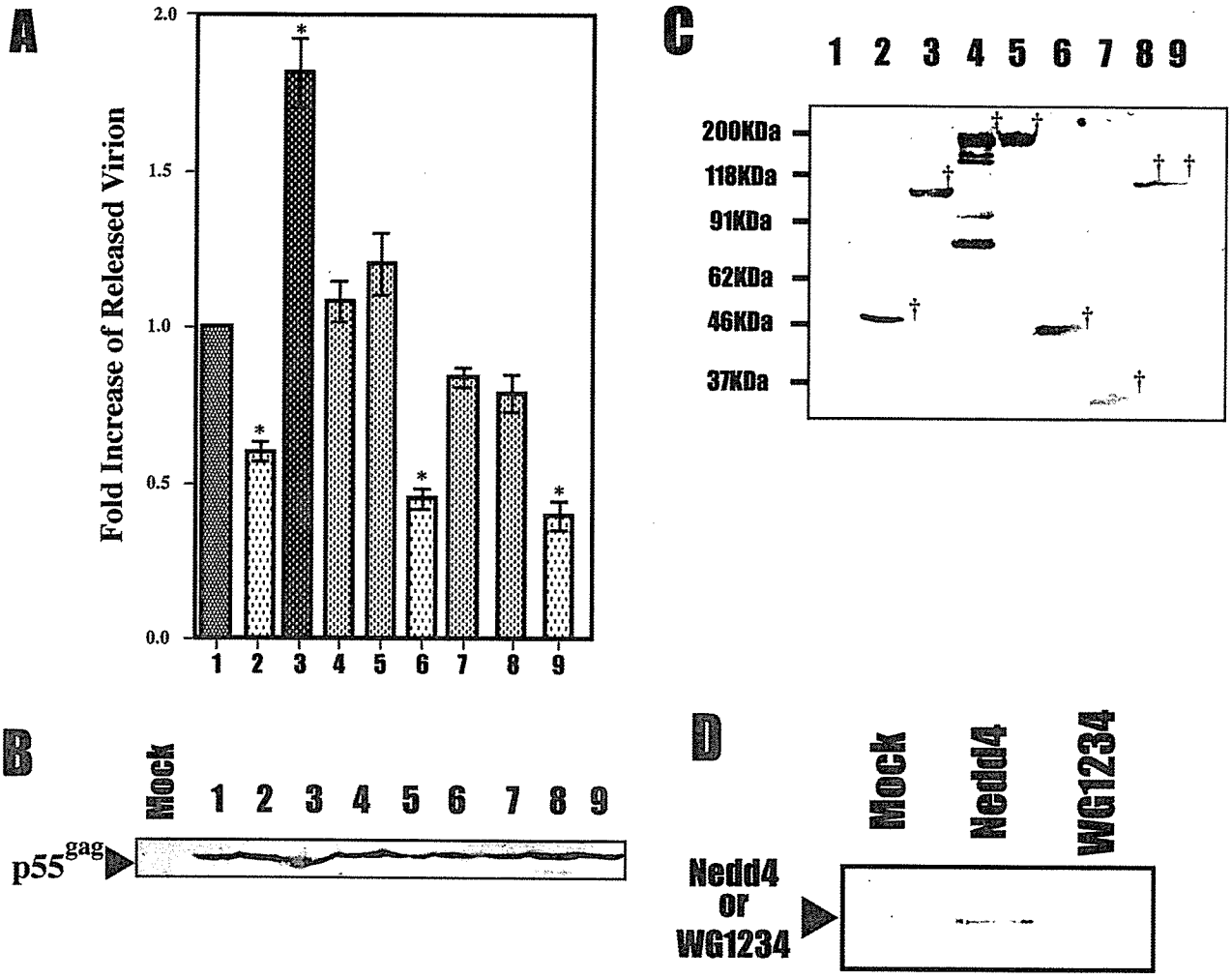

Fig. 3. Effect of overexpressing E3 ligases on HTLV-1 virion release. 293T cells were transfected with pHTLV-1 K30 and the expression vectors of the following molecules: lane 1, control vector; lane 2, Tsg101; lane 3, Nedd4; lane 4, BUL1; lane 5, KIAA1301; lane 6, Nedd4WW; lane 7, BUL1WW; lane 8, Nedd4C894A; lane 9, Nedd4WG1234. (A) The Gag proteins in the virion and cell lysate were quantitated by p19 ELISA. The data are present as the ratio of virion p19/cell p19. The extent of virion budding in wild type was set to 1.0. The data represent averages and S.D. of three independent experiments. The asterisk indicates P value <0.05. The expression levels of Gag protein (B) or E3 ligases (C) in the cell lysates were examined by western blotting with the α-p24 or α-c-myc MAb, respectively. †: the corresponding protein bands. (D) Incorporation of Nedd4 into virions. VLP fractions sedimented by ultracentrifugation were analyzed by western blotting with α-c-myc.

3.3. Overexpression of Nedd4 enhances HTLV-1 budding

The PPxY motif is known to interact with the WW domain [27]. Indeed, we recently reported that the novel ubiquitin ligase BUL1 interacts with the PPPY motif of the M-PMV Gag protein through its WW domain(s) [17]. To examine the involvement of ubiquitin E3 ligase on the egress of the HTLV-1 virus, we overexpressed three kinds of E3 ligases, namely, Nedd4, BUL1 and KIAA1301. Thus, 293T cells were transfected with 0.5 μg of pHTLV-1 K30 and 2.0 μg of each myc-tagged E3 ligase expression vector. Forty-eight hours after transfection, the virions in the culture medium were collected and quantified by ELISA. The p19 levels in the medium were normalized for budding efficiency by the amount of p19 Gag in the cell lysate. Overexpression of Nedd4 enhanced HTLV-1 release, but overexpression of BUL1 and KIAA1301 had little effect on HTLV-1 budding (Fig. 3A). To check the expression levels of the Gag protein and E3 ligases in the transfected cells, we performed western blot analyses with NOR-1 and the anti-c-myc MAb 9E10, respectively. These assays showed that overexpression of the E3 ligases had no pronounced effect on Gag synthesis and stability (Fig. 3B) and that the E3 ligases were efficiently expressed (Fig. 3C). Taken together, these results suggest that Nedd4 or a Nedd4-related E3 ligase plays a critical role in HTLV-1 budding.

3.4. Effect of Nedd4 mutants on HTLV-1 release

To further analyze the regulation of HTLV-1 budding by Nedd4, we constructed several Nedd4 mutants and examined the effect of their overexpression on budding. Nedd4WW expresses only four WW domains composed of the amino acids positioned from 218 to 533. Nedd4WG1234 is a mutant

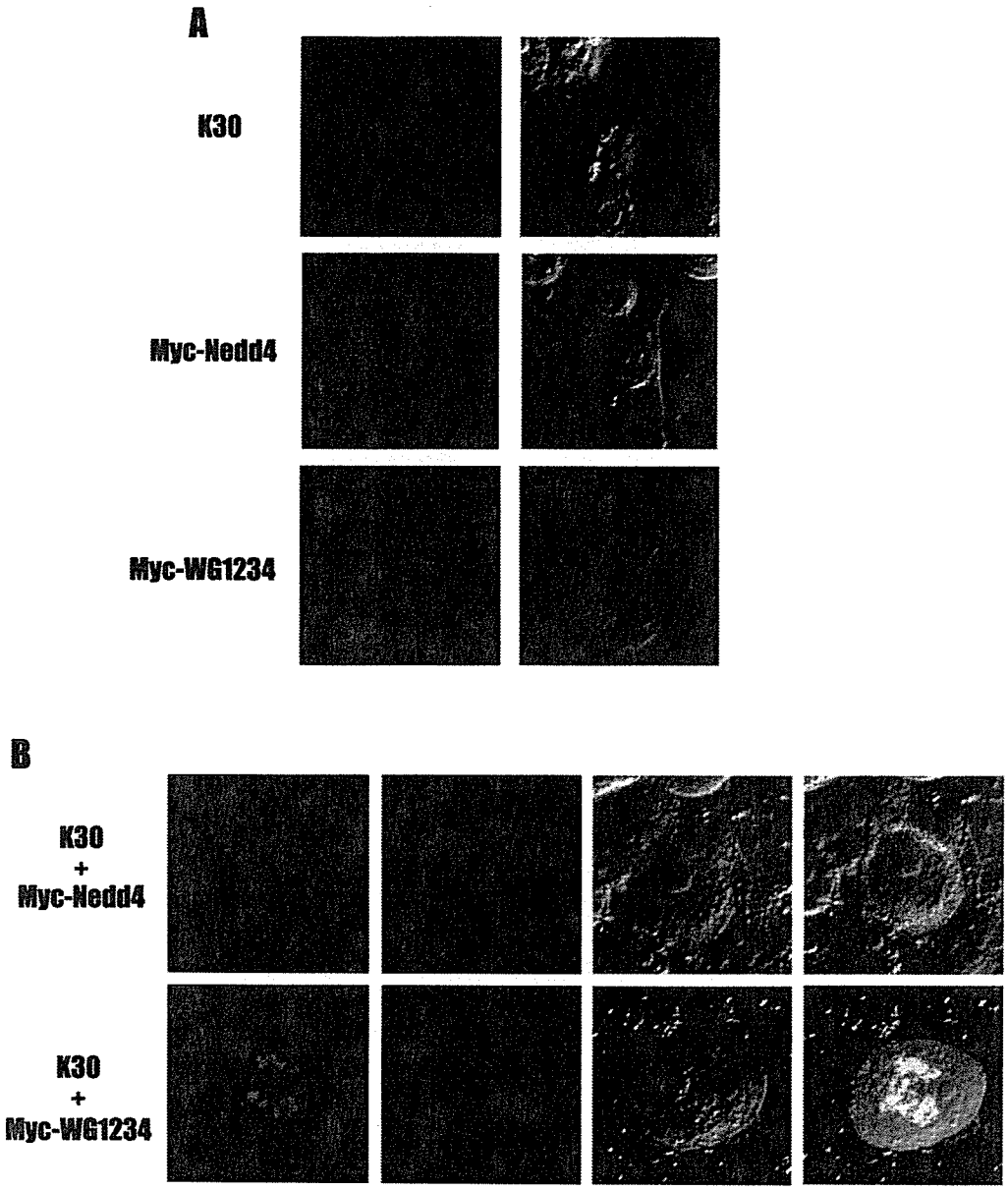

Fig. 4. Localization of HTLV-1 Gag and myc-tagged Nedd4 or Nedd4WG1234. (A) 293T cells were transfected with HTLV-1 K30 (upper) and/or myc-Nedd4 (middle) or myc-Nedd4WG1234 (lower). Gag p24 and the c-myc-tagged protein are stained red and green, respectively. (B) 293T cells were co-transfected with HTLV-1 K30 and the Nedd4 (upper) or the Nedd4WG1234 (lower) expression plasmid.

that has W–G substitutions in all four WW domains. In Nedd4C894A, the critical Cys-894 in the HECT domain has been replaced with Ala [28]. Overexpression of Nedd4WW reduced HTLV-1 release from the cells, while overexpression of BUL1WW, which contains the WW domains of BUL1, had little effect on Gag release (Fig. 3A). Thus, the Nedd4WW domain may interact more strongly with the HTLV-1 PPxY motif than with the BUL1WW domain. Nedd4C894A lost its ability to facilitate virus budding, suggesting that HECT activity is required for the budding function of this protein. Interestingly, Nedd4WG1234 inhibited virion release as much as Nedd4WW. In contrast to Nedd4, overexpression of Tsg101 inhibited the viral budding. To determine whether the release inhibition by overexpression of Tsg101 depends on the PTAP sequence of Gag or not, we transfected 293T cells with 2.0 μg of pBj–Tsg101–myc and 0.5 μg of the wild-type or ΔPTAP Gag expression vectors. Overexpression of Tsg101 reduced the release of VLPs containing ΔPTAP Gag to the same extent as wild-type Gag, (data not shown). Thus, the effect of Tsg101 is independent of interaction between Tsg101 and the PTAP sequence of HTLV-1 Gag.

3.5. Localization of HTLV-1 Gag and Nedd4

Next, to study the effect of overexpressing Nedd4 on Gag localization, we transfected 293T cells with 0.5 μg of pHTLV-1 K30 and 3.0 μg of the Nedd4 or Nedd4WG1234 expression vector and then examined them by immunofluorescence techniques. Nedd4–myc was observed in the cyto-

plasm of the cells when the cells were transfected with the Nedd4 expression plasmid alone (Fig. 4A) [28]. In the cells transfected with pHTLV-1 K30 alone, viral Gag protein was found to localize in both the cytoplasm and the nucleus (Fig. 4A). However, in the cells coexpressing Nedd4 and HTLV-1, the localization of Gag changed to the cytoplasm alone, where it colocalized with Nedd4 (Fig. 4B, upper). Interestingly, Nedd4WG1234 was observed as aggregates in the nuclear or perinuclear region (Fig. 4A) and had no effect on the localization of Gag (Fig. 4B, lower). These results suggest that HTLV-1 Gag specifically binds to the WW domain of Nedd4. This specific interaction between Nedd4 and Gag was also confirmed by the specific incorporation of Nedd4, but not Nedd4WG1234, into virions (Fig. 3D).

We also examined the subcellular localizations of BUL1, KIAA1301 and Nedd4C894A. The two E3s and the Nedd4 mutant were observed in the cytoplasm, and all altered the Gag localization to the cytoplasm to the same extent as wild-type Nedd4 (data not shown).

4. Discussion

Several enveloped viruses, including HTLV-1, MuLV, M-PMV, vesicular stomatitis virus and Ebola virus, bear both a PT/SAP and a PPxY motif in the L domain of the Gag protein [4]. A recent report [26] indicated that the PPPY sequence of HTLV-1 p19 (MA) was required for viral budding. However, they did not examine the effect of the PTAP sequence. In this report, we demonstrated that the PTAP sequence of HTLV-1 p19 was not essential for viral release and that the PPPY motif plays an important role in the budding from membrane. In contrast, the Ebola virus requires both L-domain motifs. Thus, the viruses containing both the PT/SAP motif and the PPxY motif use these L-domain motifs differently in budding. It will be interesting to analyze the functions of the L-domain motifs in the other viruses that have both sequences, as this may help us to better understand the mechanism of virus budding. It may also give clues about the evolution of these viruses.

Overexpression of Nedd4 increased the amounts of HTLV-1 virions, while Nedd4WW inhibited virion release. In addition, other E3 ligases, BUL1 and KIAA1301, had little effect on viral egress. These results suggest that Nedd4 or a Nedd4-related E3 ligase plays a critical role in HTLV-1 budding. Previously, we showed that BUL1, but not Nedd4, enhances the PPxY-mediated budding of M-PMV [17]. Thus, viruses containing a PPxY motif in the L domain seem to utilize different E3 ligases in the viral budding step.

Interestingly, Nedd4WG1234 also inhibits HTLV-1 budding, although it does not compete with endogenous Nedd4 for binding to Gag. Since the mutant was observed to aggregate in the cytoplasm, it is conceivable that Nedd4WG1234 may alter the subcellular localization of other critical cellular factors such as E2 ubiquitin ligase, which results in the inhibition of virus budding.

In the cells coexpressing Nedd4 and HTLV-1, Gag was localized to the cytoplasm only, and colocalized with Nedd4. On the other hand, overexpression of Nedd4WG1234 had no effect on Gag localization. These results indicate that Nedd4 interacts with HTLV-1 Gag via its WW domain(s). Overexpression of BUL1, KIAA1301 and Nedd4C894A also altered the Gag localization, although these E3s do not affect HTLV-1 budding. These results indicate that the interaction of an E3 ligase with the PPxY motif of Gag via the WW domains is necessary but not enough for virus budding. Thus, a region(s) other than the WW domains, such as the HECT domain, may be required to facilitate the budding function of Nedd4. Particularly, C894A mutation in Nedd4 abolished the function of this ligase in HTLV-1 viral budding, which suggests that the enzymatic activity of Nedd4 as a ubiquitin ligase may be essential for viral budding.

Overexpression of Tsg101 had an inhibitory effect on HTLV-1 budding irrespective of the presence of the PTAP motif in the Gag. Recently, Goila-Gaur et al. [29] reported that overexpression of Tsg101 inhibits HIV-1 release in a manner independent of the interaction between HIV-1 Gag and Tsg101. Taken together, overexpression of Tsg101 may inhibit HTLV-1 budding by disturbing the multivesicular body (MVB) sorting pathway. Moreover, Garrus et al. [21] consistently reported that a dominant negative mutant of VPS4, which plays an important role in the MVB sorting pathway, inhibited the budding not only of HIV-1 but also of MuLV. MuLV bears the PPxY motif as its L domain, whereas HIV-1 uses PTAP [9,10]. Thus, the MVB sorting pathway may be required for the budding of both PPxY- and PT/SAP-bearing viruses. We propose that the PPxY-dependent budding of various viruses may utilize a specific E3 ligase(s) during the first steps, after which budding is continued using a process such as the MVB sorting pathway, which is also employed by PT/SAP-bearing viruses.

Acknowledgements

We thank Kantou Nakajima, Tsubasa Ohta and Junko Hioki for their excellent technical assistance. This work was supported by grants from the Ministry of Education, Sports, Science and Technology (MEXT) of Japan, the Japan Society for the Promotion of Science (JSPS), the Japan Health Science Foundation (JHSF), and the Ministry of Health, Labour and Welfare of Japan. The infectious molecular HTLV-1 clone K30 was obtained through the AIDS Research and Reference Reagent program.

References

[1] M.A. Accola, B. Strack, H.G. Gottlinger, Efficient particle production by minimal Gag constructs which retain the carboxy-terminal domain of human immunodeficiency virus type 1 capsid-p2 and a late assembly domain, J. Virol. 74 (2000) 5395–5402.

[2] E.O. Freed, Viral late domains, J. Virol. 76 (2002) 4679–4687.

[3] M. Huang, J.M. Orenstein, M.A. Martin, E.O. Freed, p6Gag is required for particle production from full-length human immunodeficiency virus type 1 molecular clones expressing protease, J. Virol. 69 (1995) 6810–6818.

[4] O. Pornillos, J.E. Garrus, W.I. Sundquist, Mechanisms of enveloped RNA virus budding, Trends Cell Biol. 12 (2002) 569–579.

[5] V.M. Vogt, Ubiquitin in retrovirus assembly: actor or bystander? Proc. Natl. Acad. Sci. USA 97 (2000) 12945–12947.

[6] A. Patnaik, J.W. Wills, In vivo interference of Rous sarcoma virus budding by cis expression of a WW domain, J. Virol. 76 (2002) 2789–2795.

[7] B. Strack, A. Calistri, M.A. Accola, G. Palu, H.G. Gottlinger, A role for ubiquitin ligase recruitment in retrovirus release, Proc. Natl. Acad. Sci. USA 97 (2000) 13063–13068.

[8] J. Yasuda, E. Hunter, A proline-rich motif (PPPY) in the Gag polyprotein of Mason–Pfizer monkey virus plays a maturation-independent role in virion release, J. Virol. 72 (1998) 4095–4103.

[9] J. Martin-Serrano, T. Zang, P.D. Bieniasz, HIV-1 and Ebola virus encode small peptide motifs that recruit Tsg101 to sites of particle assembly to facilitate egress, Nat. Med. 7 (2001) 1313–1319.

[10] E.L. Myers, J.F. Allen, Tsg101, an inactive homologue of ubiquitin ligase e2, interacts specifically with human immunodeficiency virus type 2 gag polyprotein and results in increased levels of ubiquitinated gag, J. Virol. 76 (2002) 11226–11235.

[11] L.J. Parent, R.P. Bennett, R.C. Craven, T.D. Nelle, N.K. Krishna, J.B. Bowzard, C.B. Wilson, B.A. Puffer, R.C. Montelaro, J.W. Wills, Positionally independent and exchangeable late budding functions of the Rous sarcoma virus and human immunodeficiency virus Gag proteins, J. Virol. 69 (1995) 5455–5460.

[12] B. Yuan, S. Campbell, E. Bacharach, A. Rein, S.P. Goff, Infectivity of Moloney murine leukemia virus defective in late assembly events is restored by late assembly domains of other retroviruses, J. Virol. 74 (2000) 7250–7260.

[13] R.N. Harty, M.E. Brown, G. Wang, J. Huibregtse, F.P. Hayes, A PPxY motif within the VP40 protein of Ebola virus interacts physically and functionally with a ubiquitin ligase: implications for filovirus budding, Proc. Natl. Acad. Sci. USA 97 (2000) 13871–13876.

[14] J.M. Licata, M. Simpson-Holley, N.T. Wright, Z. Han, J. Paragas, R.N. Harty, Overlapping motifs (PTAP and PPEY) within the Ebola virus VP40 protein function independently as late budding domains: involvement of host proteins TSG101 and VPS-4, J. Virol. 77 (2003) 1812–1819.

[15] R.N. Harty, J. Paragas, M. Sudol, P. Palese, A proline-rich motif within the matrix protein of vesicular stomatitis virus and rabies virus interacts with WW domains of cellular proteins: implications for viral budding, J. Virol. 73 (1999) 2921–2929.

[16] A. Kikonyogo, F. Bouamr, M.L. Vana, Y. Xiang, A. Aiyar, C. Carter, J. Leis, Proteins related to the Nedd4 family of ubiquitin protein ligases interact with the L domain of Rous sarcoma virus and are required for gag budding from cells, Proc. Natl. Acad. Sci. USA 98 (2001) 11199–11204.

[17] J. Yasuda, E. Hunter, M. Nakao, H. Shida, Functional involvement of a novel Nedd4-like ubiquitin ligase on retrovirus budding, EMBO Rep. 3 (2002) 636–640.

[18] O. Pornillos, S.L. Alam, D.R. Davis, W.I. Sundquist, Structure of the Tsg101 UEV domain in complex with the PTAP motif of the HIV-1 p6 protein, Nat. Struct. Biol. 9 (2002) 812–817.

[19] L. VerPlank, F. Bouamr, T.J. LaGrassa, B. Agresta, A. Kikonyogo, J. Leis, C.A. Carter, Tsg101, a homologue of ubiquitin-conjugating (E2) enzymes, binds the L domain in HIV type 1 Pr55(Gag), Proc. Natl. Acad. Sci. USA 98 (2001) 7724–7729.

[20] D.G. Demirov, A. Ono, J.M. Orenstein, E.O. Freed, Overexpression of the N-terminal domain of TSG101 inhibits HIV-1 budding by blocking late domain function, Proc. Natl. Acad. Sci. USA 99 (2002) 955–960.

[21] J.E. Garrus, U.K. von Schwedler, O.W. Pornillos, S.G. Morham, K.H. Zavitz, H.E. Wang, D.A. Wettstein, K.M. Stray, M. Cote, R.L. Rich, D.G. Myszka, W.I. Sundquist, Tsg101 and the vacuolar protein sorting pathway are essential for HIV-1 budding, Cell 107 (2001) 55–65.

[22] I. Le Blanc, A.R. Rosenberg, M.C. Dokhelar, Multiple functions for the basic amino acids of the human T-cell leukemia virus type 1 matrix protein in viral transmission, J. Virol. 73 (1999) 1860–1867.

[23] H. Wang, K.M. Norris, L.M. Mansky, Analysis of bovine leukemia virus gag membrane targeting and late domain function, J. Virol. 76 (2002) 8485–8493.

[24] J. Yasuda, M. Nakao, Y. Kawaoka, H. Shida, Nedd4 regulates egress of Ebola virus-like particles from host cells, J. Virol. 77 (2003) 9987–9992.

[25] Y. Tanaka, B. Lee, T. Inoi, H. Tozawa, N. Yamamoto, Y. Hinuma, Antigens related to three core proteins of HTLV-I (p24, p19 and p15) and their intracellular localizations, as defined by monoclonal antibodies, Int. J. Cancer 37 (1986) 35–42.

[26] I. Le Blanc, M.C. Prevost, M.C. Dokhelar, A.R. Rosenberg, The PPPY motif of human T-cell leukemia virus type 1 Gag protein is required early in the budding process, J. Virol. 76 (2002) 10024–10029.

[27] L. Garnier, J.W. Wills, M.F. Verderame, M. Sudol, WW domains and retrovirus budding, Nature 381 (1996) 744–745.

[28] T. Anan, Y. Nagata, H. Koga, Y. Honda, N. Yabuki, C. Miyamoto, A. Kuwano, I. Matsuda, F. Endo, H. Saya, M. Nakao, Human ubiquitin-protein ligase Nedd4: expression, subcellular localization and selective interaction with ubiquitin-conjugating enzymes, Genes Cells 3 (1998) 751–763.

[29] R. Goila-Gaur, D.G. Demirov, J.M. Orenstein, A. Ono, E.O. Freed, Defects in human immunodeficiency virus budding and endosomal sorting induced by TSG101 overexpression, J. Virol. 77 (2003) 6507–6519.

Available online at www.sciencedirect.com
SCIENCE DIRECT
Microbes and Infection 6 (2004) 715–724
Microbes and Infection
www.elsevier.com/locate/micinf

Original article

Role of Nup98 in nuclear entry of human immunodeficiency virus type 1 cDNA

Hirotaka Ebina [a], Jun Aoki [a], Shunsuke Hatta [a], Takeshi Yoshida [a], Yoshio Koyanagi [b,*]

[a] Department of Virology, Tohoku University Graduate School of Medicine, Sendai 980-8575, Japan
[b] Laboratory of Viral Pathogenesis, Institute for Virus Research, Kyoto University, 53 Shougoin-kawahara machi, Sakyou-ku, Kyoto 606-8507, Japan

Received 18 February 2004; accepted 7 April 2004

Available online 24 May 2004

Abstract

Human immunodeficiency virus type 1 (HIV-1), like other lentiviruses, can infect non-dividing cells. The lentiviruses are most likely to have evolved a nuclear import strategy to import HIV-1 cDNA and viral protein complex through the nuclear pore complex (NPC) formed by nucleoporin proteins (Nup). In this study, we found that synthesis of integrated and 2LTR but not full-length form of HIV-1 cDNA was clearly impaired in culture via transduction of vesicular stomatitis virus matrix protein (VSV M), an inhibitor protein, through binding to the phenylalanine-glycine (FG) repeat region of Nup98. The impairment of synthesis of integrated and 2LTR DNA with VSV M was restored by ectopic overexpression of Nup98. A series of experiments using Nup98-depleted NPC by the small interfering RNA (siRNA) technique showed specific impairment of NPC structure and some functions, including nuclear import of HIV-1 cDNA. Our results suggest that Nup98 on the NPC specifically participates in the nuclear entry of HIV-1 cDNA following HIV-1 entry.
© 2004 Elsevier SAS. All rights reserved.

Keywords: Nucleoporin; NPC; HIV-1; Nuclear import

1. Introduction

The Retroviridae family of viruses can reverse transcribe their RNA genome into cDNA and then integrate the cDNA into host chromosomes. The lentiviruses (e.g. HIV) are distinguished by their ability to infect non-dividing cells, whereas the gamma-retroviruses (e.g. Moloney murine leukemia virus) require nuclear membrane dissolution to access the host cell DNA [1]. Thus, the lentiviruses are most likely to have evolved a nuclear import strategy, which allows their cDNA to cross the nuclear membrane independently of mitosis. In the case of human immunodeficiency virus type 1 (HIV-1), mitosis-independent replication was initially shown in terminally differentiated macrophages in vitro [1–3]. The mitosis-independent replication of HIV has also enabled the generation of integration-competent gene transfer vectors with promising therapeutic applications in a variety of non-dividing cellular hosts, including neurons [4], myocytes [5], and retinal cells [6]. To facilitate integration into a host DNA, a preintegration complex (PIC) is generated in the cytoplasm immediately after completion of reverse transcription. The PIC can be isolated successfully from in vitro freshly HIV-1-infected or HIV vector-infected cells and was recently shown to have the ability to traverse the nuclear pore complex (NPC) [1,7]. The NPCs serve as the conduits for bi-directional transport of macromolecules. Translocation across the NPC into the nucleus and from the nucleus into the cytoplasm is governed by a class of proteins known as importins and exportins (transport receptors), respectively. Both are members of the karyopherin family. The transport receptors engage the appropriate import or export signals and mediate their transport [8,9]. The PIC contains a double-strand linear cDNA as well as at least four viral proteins: matrix (MA), reverse transcriptase (RT), integrase (IN), and viral protein R (VPR), and has a diameter of approximately 56 nm, which greatly exceeds the 25 nm central channel of the NPC [1,7,10]. The NPC has a large supramolecular structure formed of ~50 unique proteins in eukaryotic cells, termed nucleoporins (Nup) [8,9,11,12]. High-resolution electron microscopic images of NPCs reveal an eightfold

* Corresponding author. Tel.: +81-75-751-4811; fax: +81-75-751-4812.
E-mail address: ykoyanag@virus.kyoto-u.ac.jp (Y. Koyanagi).

© 2004 Elsevier SAS. All rights reserved.
doi:10.1016/j.micinf.2004.04.002

symmetric structure, formed by nuclear and cytoplasmic rings and central spoke complex. The Nups often contain multiple phenylalanine-glycine (FG) dipeptide repeats clustered in domains, which in vertebrates are glycosylated by addition of *O*-linked *N*-acetylglucosamine (GlcNAc). Some of these Nups are localized asymmetrically at the NPC [9,11]. The asymmetric distribution of nucleoporins and the different affinities for import and export complexes may be important in determining the direction of transport [13,14]. Recent studies reported that importin 7 is involved in the nuclear entry of HIV-1 PIC as one of the main transport receptors [15]. However, the steps involved in the NPC remain largely undefined. In the present study, we show that nuclear import of HIV-1 cDNA requires NPC, and Nup98 has a role in nuclear entry of HIV-1 cDNA.

2. Materials and methods

2.1. Chemical treatment

Aphidicolin (APH) (Sigma Chemical Co., St. Louis, MO, USA), actinomycin D (ActD) (Sigma), zidovudine (AZT) (Sigma) or leptomycine B (LMB) (Sigma) was used. APH treatment (5 μg/ml) started 24 h before HIV-1 vector infection. AZT treatment started at the time of infection. LMB was added 2 h after infection. ActD was added 5 h after infection. DNA was extracted 24 h after infection.

2.2. Transfection

Human 293T cells were maintained in D-MEM containing 10% fetal calf serum (FCS). 293T cells were transfected with vesicular stomatitis virus matrix protein (VSV M)-, Nup98- or small interfering RNA (siRNA)-expressing DNA using calcium phosphate methods.

2.3. Quantitative polymerase chain reaction (PCR) assay

For the detection and quantification of individual forms of HIV-1 DNA, full-length/1LTR circle, 2LTR circle and integrated forms, we used a set of primer pairs and fluorogenic probes, as described previously [16,17]. PCR was performed using an ABI PRISM 7700 sequence detection system (PE-Applied Biosystems, Foster City, CA, USA) and TaqMan Universal PCR Master Mix (PE-Applied Biosystems). Cycling conditions included a hot start (50 °C for 2 min, 95 °C for 10 min), followed by 40 cycles of denaturation (95 °C for 15 s) and extension (60 °C for 1 min). To measure the integrated DNA, an *Alu*-sequence-specific sense primer and an antisense HIV-specific primer were used in the first PCR and subsequently 1000-fold diluted products were subjected to real-time PCR assay for measurement of R/U5 DNA, as described previously [16,17].

2.4. Cell-cycle analysis

Cell-cycle progression was examined by single-color flow cytometric analysis of the DNA content stained with 50 μg/ml of propidium iodine (Sigma).

2.5. DNA constructs and recombinant protein expression

Small interference RNA (siRNA)-expressing plasmid DNAs were constructed using the method described by Miyagishi and Taira [18]. The sequences inserted in the *Bfu*AI site of pU6i cassette, immediately downstream of the U6 promoter, were as follows: Nup98-targeted siRNA (siN98), 5′-CACC**GAATATGAAAG*T*AAGTT*A*TTA**TAGAATTACATCAAGGGAGAT**TAGTGACTTGCTTTCATATTC**-TTTTTATGC-3′; firefly luciferase-targeted siRNA (siLuc), 5′-CACC**GTGCG*T*TG*T*TGGTG*TT*AA*T*CC**ATCTCCCTTGATGTAATTCTA**GGGTTGGCACCAGCAGCGCAC**-TTTTTATGC-3′. Bold-lettered nucleotides are the siRNA sequences, italic nucleotides are mutated, and underlined nucleotides are loop sequences. The siRNA-expressing DNA fragment was also inserted into the *Eco*RI site of a lentivirus vector DNA, pCS-CDF-EH2K^k, and an enhanced green fluorescence protein (EGFP) fragment between the *Age*I and *Xho*I sites of pCS-CDF-EG-PRE [19] was replaced with a H-2K^k fragment (Daiichi pure chemicals, Tokyo, Japan).

HA-tagged human Nup98-expressing plasmid DNA (p37R-HANup98) and EGFP-fused VSV M-expressing DNA (pEGFPN3-M) [20] were kindly provided by Dr. Elisa Izaurralde (European Molecular Biology Laboratory). A *Bss*HII-*Xho*I DNA fragment covering the coding region of HA-tagged human Nup98 region was cloned into a site downstream of CMV promoter in pcDNA3.1/Zeo (+) (Invitrogen, Carlsbad, CA, USA) (pcDNup98). Alanine substitutions from Asp-Thr-Tyr at the position of VSV M 52–54 [VSV (M)] were introduced using an oligonucleotide-directed in vitro mutagenesis system (Quickchange site-directed mutagenesis, Stratagene, San Diego, CA, USA). DsRed-fusion recombinant protein with NLS, U1A and rpL23a was produced in *Escherichia coli*. A double-strand synthetic nucleotide of SV40 NLS (5′-CCA TGC ATA TGC CAA AAA AGA AGA GAA AGG TTG-3′) and PCR-amplified DNA fragment of U1A (1–486), or rpL23a (1–486) from mRNA of HeLa cells was cloned into the *Sma*I or *Sal*I-*Bam*HI sites of pDsRed1-N1 (Clontech, Palo Alto, CA, USA), and then a *Sal*I-*Not*I fragment was inserted in the *Sal*I-*Not*I site of pGEX-4T-2 (Amersham Pharmacia Biotech, Piscataway, NJ, USA). *E. coli* ER2566 (New England Biolabs Inc., Beverly, MA, USA) was used, and recombinant proteins were purified on glutathione sepharose 4 Fast Flow (Amersham) by standard protocols, as previously described [21].

2.6. Reverse-transcription PCR

Total RNA was extracted from transiently transfected cells by using a RNeasy RNA-preparation Kit (Qiagen, KJ

Venlo, The Netherlands). Reverse transcription and PCR were carried out using a SuperScript One-Step RT-PCR with Platinum Taq (Invitrogen). We used the following primers to detect the specific transcripts: for Nup107, 5′-AAACGCGGTAGCTAAACTGCA-3′, 5′-ACCACCAGCTGACTTTGTCGA-3′; for Nup214, 5′-CTTGCCACGAAAACCGTGA-3′, 5′-CAACCCGCAGTCCTGAAAA-3′; for p62, 5′-CAGACACCGACGGATTTGCTT-3′, 5′-TGGATGTTGTTGTGGAGGTGC-3′; for Nup98, 5′-TCTCATCCCAAAACAATGCCTT-3′, 5′-AAACAAAGATGCCTGTCCAGCA-3′; for Nup153, 5′-TGACAATGAAGAGCCAAAGTGT-3′, 5′-TAGGAGTTGTTCCAGAGCCAAA-3′. TaqMan GAPDH Control Reagents (PE-Applied Biosystems) were used as primer sets for glyceraldehyde 3-phosphate dehydrogenase (GAPDH). Fifty nanograms of template RNA and 10 pmol of specific primers were used. The efficiency of PCR amplification was roughly in the linear range, as determined by preliminary test with increasing number of cycles. Finally, the PCR products were analyzed by agarose gel electrophoresis using standard techniques.

2.7. Virus vector infection

For HIV-1 vector preparation, a replication-incompetent EGFP-expressing lentivirus (pCS-CDF-CG-PRE) or siRNA-expressing lentivirus was co-transfected into 293T cells along with VSV G-expressing plasmid (pVSV G), HIV-Gag-Pol-expressing plasmid (pRRE) and Rev-expressing plasmid (pRSV-Rev) as described before [6,19]. Three days after transfection, the culture supernatants were cleared by filtration and concentrated through centrifugation at 6000 × *g* for 16 h at 4 °C. The transducing unit (TU) was determined by measurement of EGFP-, or H-2K^k-expressing cells using flow cytometry. Phycoerythrin-labeled anti-mouse H-2K^k monoclonal antibody (mAb) (Cedarlane, Ontario, Canada) was used. Cells were analyzed on FACS SCAN, using Cell Quest software (BD PharMingen, San Diego, CA, USA). Treatment with DNaseI (20 μg/ml) was performed to remove plasmid DNA in the virus stocks. Heat-inactivated (65 °C, 30 min) virus liquid was used as negative control for HIV DNA quantification in infected cells. APH-treated MT-2 cells or 293T cells (2×10^5 cells) were infected with HIV-1 vector (4×10^5 TU). Two hundred thousand 293T cells were transfected with VSV M- or Nup98-expressing DNA and then 24 h later, infected with HIV-1 vector (4×10^5 TU). Two hundred thousand 293T cells were transfected with siRNA-expressing DNA and then 72 h later, infected with HIV-1 vector (4×10^5 TU). The amount of viral DNA was measured by the quantitative PCR assay 24 h after infection, as described above. HeLa cells (1×10^5 cells), grown on cover-slips, were infected with siRNA-expressing HIV-1 vector at multiplicity of infection (m.o.i.) of 1. The cells were analyzed 96 h later by immunofluorescence, immunoblotting or nuclear import assay.

2.8. Immunofluorescence analysis

HeLa cells, grown on cover-slips, were washed twice with phosphate-buffered solution (PBS) and fixed in 4% (vol/vol) paraformaldehyde/PBS for 15 min at room temperature. The cells were permeabilized with 0.2% Triton X-100/PBS for 5 min. After blocking with 5% bovine serum albumin (BSA)/0.1% Triton X/PBS for 1 h, the cells were incubated with an NPC-specific mouse mAb, mAb414 (BabCO, Berkeley, CA, USA) or anti-Nup98 polyclonal antibody (C-16) (Santa Cruz Biotechnology Inc., Santa Cruz, CA, USA) at 4 °C overnight. Cells were washed three times with 0.05% Triton X/PBS and then incubated with Alexa 594-conjugated goat anti-mouse IgG antibody (Molecular Probes, Eugene, OR, USA) or fluorescein isothiocyanate (FITC)-conjugated donkey anti-goat IgG antibodies (Chemicon, Temecula, CA, USA) for 1 h. Cells were washed three times with 0.05% Triton X/PBS, mounted in Vectashield mounting medium for fluorescence (Vector Laboratories, Burlingame, CA, USA) and analyzed with a Leica QFluoro system. The cells were also stained with Hoechst 33342 (Molecular Probes).

2.9. Nuclear import assay

HeLa cells grown on cover-slips were washed in PBS and permeabilized for 5 min on ice in 50 μg/ml digitonin (Sigma)/transport buffer (20 mM Hepes– NaOH, pH 7.3, 110 mM CH_3COOK, 2 mM $(CH_3COO)_2Mg$, 5 mM CH_3COONa, and 2 mM dithiothreitol). After washing three times with transport buffer, cells were incubated at 30 °C for 30 min in the presence of energy-regenerating system (1 mM ATP, 1 mM GTP, 10 mM creatine phosphate, and 20 U/ml creatine phosphokinase), 3 μM DsRed-labeled recombinant protein, and cytoplasmic extract from 2×10^5 HeLa cells. Samples were washed three times in transport buffer, fixed on ice for 30 min with 1% formalin/transport buffer and analyzed with a Leica QFluoro system.

2.10. Immunoblotting

293T cells were co-transfected with an HA-tagged human Nup98-expressing plasmid DNA (pcDNup98) and a siRNA-expressing plasmid (siN98 or siLuc). Three days after transfection, the cells were washed twice and lysed in RIPA buffer (0.5% NP-40 in 20 mM Tris–HCl [pH 8.2], 0.15 M NaCl, 5 mM iodoacetamide, and 1 mM phenylmethylsulfonyl fluoride). After loading on SDS/PAGE, polypeptides were transferred to Immobilion Transfer Membranes (Millipore, Billerica, MA, USA), the level of Nup98 was determined using a goat anti-Nup98 polyclonal antibody (C-16), biotin-conjugated rabbit anti-goat IgG (Chemicon) and then incubated with horseradish peroxidase (HRP)-conjugated streptavidin (Zymed, San Francisco, CA, USA). The filter generated from HeLa cells infected with siRNA-expressing

HIV-1 vector as described above was also incubated with mAb414 (mainly reactive against p62), biotin-conjugated horse anti-mouse IgG (VECTOR) and HRP-conjugated streptavidin. The specific bands were detected using Western Lighting Chemiluminescence Reagent (Perkin–Elmer Life Science, Boston, MA, USA). For detection of Nup98-VSV M complex, 293T cells were co-transfected with Nup98-expressing plasmids (pcDNup98) and EGFP-fused VSV M-expressing plasmid DNA (pEGFPN3-M) or the mutant [VSV M(D)]. Two days after transfection, the cells were lysed in triple detergent lysis buffer (1% NP-40, 0.1% SDS, 0.5% sodium deoxycholate in 50 mM Tris–HCl [pH 8.0], 0.15 M NaCl, 1 μg/ml aprotinin, 1 mM phenylmethylsulfonyl fluoride), and a mouse anti-HA mAb (F-7) (Santa Cruz) was added. After incubation for 12 h at 4 °C with protein G-sepharose (Amersham), the precipitate was washed three times with triple detergent lysis buffer, and the bound proteins were eluted by 1× sample buffer (1.71% SDS in 175 mM Tris–HCl [pH 6.8], 5% glycerol, 1% 2-mercaptoethanol) at 37 °C for 30 min. The samples were loaded on SDS/PAGE and transferred to Immobilon Transfer Membranes. For detection of the Nup98, a goat anti-Nup98 polyclonal antibody (C-16) (Santa Cruz) and biotin-conjugated rabbit anti-goat IgG (Chemicon) were used. For detection of VSV M, a rabbit anti-GFP polyclonal antibody (Santa Cruz) and biotin-conjugated donkey anti-rabbit IgG (Chemicon) were used.

2.11. Statistical analysis

All data were expressed as mean ± standard deviations (S.D.). Differences between groups were examined for statistical significance using the Welch's *t*-test. A P value less than 0.05 denoted the presence of a statistically significant difference.

3. Results

3.1. Efficient nuclear import of HIV-1 cDNA in infected cells

It has been shown that HIV and HIV-based lentivirus vectors efficiently infect non-dividing cells [2,6]. To determine the integration efficiency in dividing and non-dividing cells, we prepared cell-cycle-arrested T cell culture using MT-2 cells treated with APH, an inhibitor of DNA polymerase α. Under this condition, cell-cycle was confirmed to be stopped at G1 phase from flow cytometric analysis (Fig. 1A). The same numbers of treated (arrested) or untreated (proliferating) cells were infected with the same amounts of HIV-1 vector and the arrested culture was further maintained in the presence of APH. Since in this experiment we used a single-round infection system, we could estimate the precise efficiency of reverse transcription, nuclear translocation as well as integration. Total DNA was extracted 24 h after infection and a set of real-time PCR assay was performed [16,17]. Using this assay, we were able to measure the full-length/1LTR circle, 2LTR circle and integrated forms of HIV-1 cDNA, respectively. Since the 2LTR circle and integrated forms are found only in nucleus after HIV infection [3,22], we could estimate the efficiency of nuclear entry as well as integration of HIV-1 cDNA. Fig. 1B shows that the levels of integrated, 2LTR and full-length/1LTR circle form in proliferating cultures were higher than those in arrested cultures, because the numbers of the cells were two to three times greater in proliferating culture. However, significant amounts of integrated ($4.2 \times 10^5 \pm 5.4 \times 10^4$ copies per culture) and 2LTR ($1.5 \times 10^5 \pm 1.5 \times 10^3$ copies per culture) form DNA were found in the arrested culture (Fig. 1B). Similar results were also obtained in APH-treated 293T cells (data not shown). These data correspond well with the previously reported findings of the high susceptibility of APH-treated cells to HIV-1 [3,22]. Importantly, the ratios of integrated form and 2LTR form to full-length/1LTR form were similar in the proliferating (integrated; 0.108 ± 0.024, 2LTR; 0.022 ± 0.002, full-length/1LTR; 1.0) and the arrested cultures (integrated; 0.09 ± 0.011, 2LTR; 0.031 ± 0.001, full-length/1LTR; 1.0), respectively, strongly suggesting that HIV-1 cDNA efficiently traverse NPC, depending on the active nuclear import machinery in not only non-dividing cells but also proliferating cells.

3.2. Inhibition of HIV-1 cDNA import with a Nup98-specific inhibitor

Next, to examine the specificity of our real-time PCR assay and the associated molecules in nuclear entry of HIV-1 cDNA, we prepared HIV reverse transcription-inhibited (AZT-treated), transcription-blocked (ActD-treated), or CRM1-dependent nuclear export-inhibited (LMB-treated) 293T cell cultures. As expected, AZT significantly inhibited the appearance of all forms of DNA (Fig. 2A a–c). Although dose-dependent inhibition of integration was found in ActD- or LMB-treated cultures, significant accumulation of the 2LTR form was also found (Fig. 2A f and i), suggesting that newly synthesized proteins as well as CRM1-dependent exported proteins may be required for the efficient integration but not nuclear entry of HIV-1 cDNA. To examine whether specific Nups are required for HIV infection, we used VSV M protein, a specific inhibitor protein against Nup98. It has been shown that Nup98 is involved in the nuclear import of some proteins as well as the export of RNA, and its function is specifically impaired in the presence of VSV M protein [20]. The VSV M binds a region within residues 66–515 of Nup98 that encompasses most of the FG repeats, the hRAE1/Gle2 binding site or GLEBS-like motif [23], and most of the predicted glycosylation sites of the Nups. Through these sites, Nup98 was able to interact with three

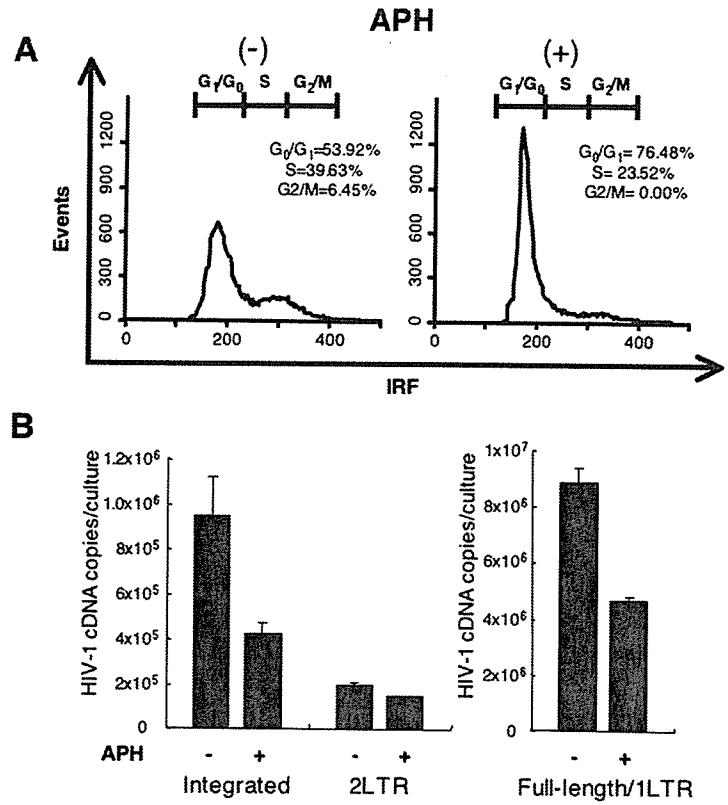

Fig. 1. Efficient nuclear entry of HIV-1 cDNA in arrested cells. (A) Cell-cycle analysis of APH-treated and -untreated cells. MT-2 cells were incubated for 24 h without (–) or with (+) APH, and then analyzed for DNA content by flow cytometry of proridium iodide-stained nuclei. Representative flow cytometry data from one of three independent experiments is shown. (B) Quantification of HIV-1 cDNA after HIV-1 vector infection in APH-treated and -untreated cells. Number of viral DNA copies per culture (baseline cell number is 2×10^5 cells) is indicated. APH-treated or -untreated MT-2 cells were infected with HIV-1 vector, and cultured without (–) or with (+) APH for another 24 h, respectively. Then, DNA was extracted and subjected to PCR assay. Results are mean ± S.D. of three independent experiments.

putative Nup98 partners: RAE1 [23], CRM1 [24], and TAP [25]. VSV M-mediated inhibition was not observed in a site-directed mutant (residue 52–54), termed VSV M(D) [20]. We used the VSV M as a specific inhibitor of the Nup98 function. An obvious impairment of integrated and 2LTR but not full-length DNA was found in only the wild-type but not the mutant VSV M(D)-transfected culture (Fig. 2B). This impairment was restored with ectopic overexpression of Nup98 (pcDNup98) (Fig. 2B, lane 5). Western blotting indicated that the overexpressed Nup98 was co-precipitated with VSV M but not VSV M(D) protein (Fig. 2C), suggesting that the overexpressed Nup98 absorbed VSV M protein, and the Nup98 function was recovered. Thus, Nup98 may have a role in nuclear import of HIV cDNA.

3.3. Depletion of Nup98 by siRNA

Next, to examine directly the involvement of Nup98 in HIV-1 cDNA nuclear import, Nup98 was depleted by the siRNA technique. After transfection with Nup98-specific siRNA-expressing plasmid, mRNA expression of Nup98 as well as Nup96, generated from the same precursor transcripts of Nup98 [26], but not other Nups such as p62, Nup107, Nup153, and Nup214, were specifically inhibited (Fig. 3A). It was also confirmed that the level of ectopic Nup98 protein expression was inhibited with the siRNA-expressing plasmid as it was lower than that in its endogenous expression (Fig. 3B). Immunofluorescence analysis using an anti-Nup98 antibody also confirmed the significant inhibition of Nup98 expression on nuclear membrane in the Nup98 siRNA-targeted HeLa cells using a siRNA-expressing lentivirus vector (Fig. 3C, upper panel). We further examined the distribution of NPC components using mAb414, an antibody known to interact with many FG-containing Nups, mainly p62 and to a less degree, Nup153, Nup214, and Nup358 but not Nup98. The Nup98 siRNA-transduced cells exhibited weak mAb414-labeling intensity at the nuclear rim and shift of labeling to the cytoplasm, probably cytoplasmic annulate lamellae (Fig. 3C, lower panel). However, the total amount of p62 (main component of NPC) was similar in both Nup98-siRNA-targeted or control cultures (Fig. 3D). A previous study using Nup98 knockout mice indicated that Nup98 is essential for rapid cell proliferation but dispensable for basal cell growth and some specific destruction of NPC component [27]. The Nup98-knockout cell was reported to have a thin nuclear envelope as well as many cytoplasmic annulate lamellae. Our Nup98-siRNA-targeted cells had similar structures. It was also reported that the mutant pores of the knockout cells were clearly impaired in in vitro transport

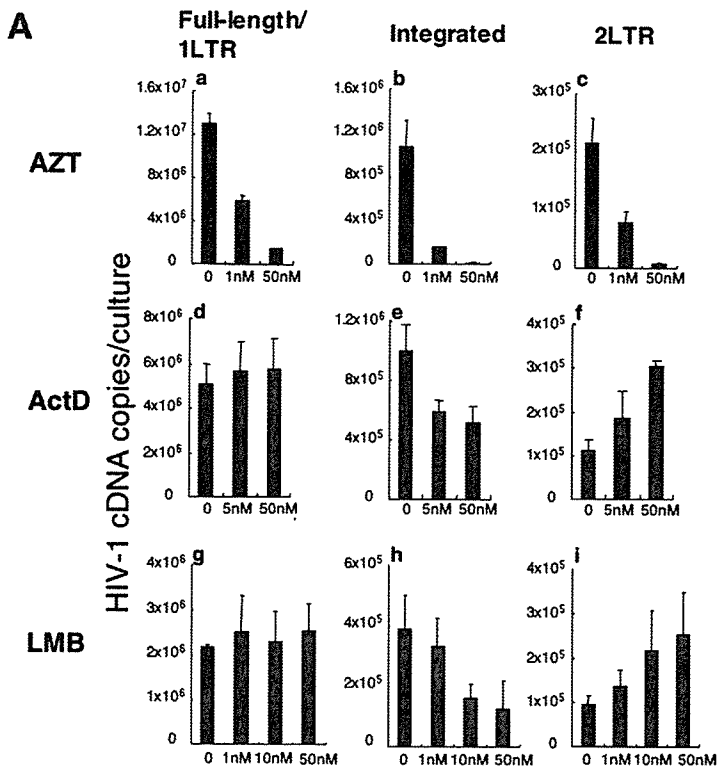

Fig. 2. Measurement of nuclear entry and integration of HIV-1 cDNA in cells treated with inhibitors. (A) Inhibition of HIV-1 cDNA appearance with chemical treatment. 293T cells were infected with HIV-1 vector at a m.o.i. of 0.5–1 and cultured in the presence of AZT, ActD, or LMB at indicated doses. HIV-1 cDNA copy numbers in AZT-treated (a, b, c), ActD-treated (d, e, f) and LMB-treated (g, h, i) cultures are indicated. Left panels (a, d, g) indicate full-length/1LTR circle, middle panels (b, e, h) indicate integrated forms, and right panels (c, f, i) indicate 2LTR circle, respectively. (B) Inhibition of nuclear entry of HIV-1 cDNA with VSV M transduction. Full-length/1LTR circle, 2LTR circle and integrated forms of HIV-1 cDNA in VSV M-transduced cultures are indicated. 293T cells were transfected with VSV M- or VSV M(D)-expressing DNA (lane 3, 4). pcDNA3.1/Zeo(+) was used as control (lane 2). The VSV M-transduced cells were also transfected together with Nup98-expressing DNA (lane 5). Then, these cells were infected with HIV-1 vector 24 h later. Total DNA was extracted 24 h after infection. Results are mean ± S.D. of three independent experiments (A and B). $*P < 0.05$ was judged as a significant difference using Welch's t-test. (C) Binding of Nup98 to VSV M protein. Western blotting using anti-GFP antibody (whole lysate) indicates VSV M or VSV M(D) expression. Binding of ectopically expressed Nup98 to VSV M protein was shown by immunoprecipitation with anti-HA antibody (anti-HA IP) and Western blotting using anti-Nup98 or anti-GFP antibodies. Results of one representative experiment from three independent experiments are shown.

assays with nuclear localization signal (NLS) of SV40 or M9 import signal (mediated by importin α/β and importin β2, respectively), while the ability of the mutant pore to import ribosomal protein L23a (mediated by either importin β, importin β2, importin β3 or importin 7) [28] and splice some protein U1A (independent of cytosolic transport factors) was intact [27]. To examine the import ability of Nup98-siRNA-targeted pores, we performed a set of import assays. These experiments were performed in a transport buffer containing specific soluble transport receptors, an energy-regenerating system, and a DsRed-labeled protein acting as a substrate for import into the nuclei of digitonin-permeabilized cells [29]. The nuclear import with an SV40 NLS import signal was substantially lower in the Nup98-depleted cells than in control cells. In contrast, translocation of rpL23 or U1A was similar in Nup98-depleted and control cells (Fig. 2E, F). These results indicated that protein import pathways were similarly impaired in both Nup98-depleted human cells using siRNA and Nup98-knockout cells, although the level of impairment of NLS in the Nup98-depeleted cells using siRNA seems to be lower than that in knockout cells.

3.4. A role of Nup98 in HIV-1 cDNA import

Finally, Nup98-depleted cells using a siRNA-expressing plasmid DNA were infected with HIV-1 vector, and the levels of integrated, 2LTR, and full-length/1LTR forms of HIV-1 cDNA were measured. Obvious reductions of integrated and 2LTR but not full-length DNA were noted in the Nup98-depleted culture. In contrast, in culture transfected with a control siRNA-expressing DNA targeted for luciferase (si-Luc), the levels of integrated, 2LTR and full-length DNA were still high (Fig. 3G). These findings suggest that Nup98 in the NPC participates in the nuclear entry of HIV-1 cDNA.

4. Discussion

The major finding of the present study is that Nup98 has an important role in the nuclear import of HIV-1 cDNA, based on a series of experiments using an inhibitor (VSV M protein) and the siRNA technique for Nup98. The role of

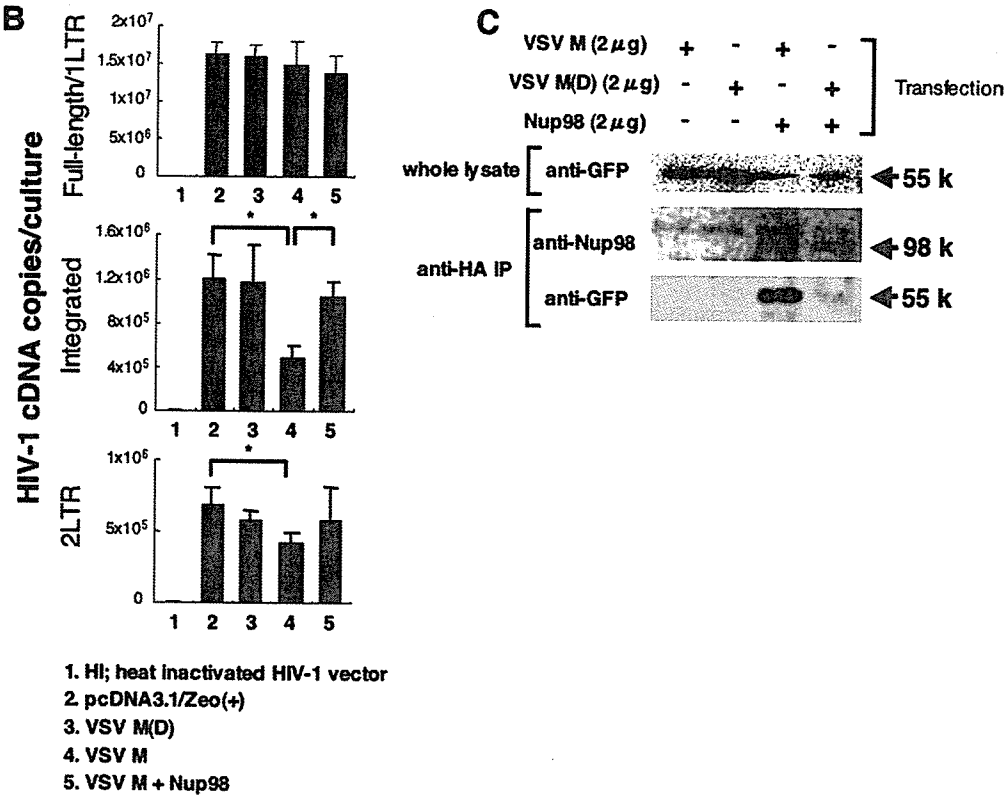

Fig. 2. *(continued)*

NPC in virus replication has been shown previously in other virus families [30]. It was reported that the import process of adenovirus type 2 DNA through NPC involves Nup214 as well as histone H1 [31]. Adenovirus capsid docks on Nup214, probably involving recruitment of importin 7/β heterodimer to the capsid, and effective disassembly at NPC activates the entry of viral DNA into nuclei [31]. Herpes simplex virus capsid docks on NPC, probably mediated by importin β alone, and undergoes a conformational shift that results in extrusion of viral DNA genome into nucleus through NPC [32]. It is possible that specific molecular events may occur at NPC during the nuclear entry of HIV-1 cDNA [15].

We recently transduced a siRNA-expressing DNA for Nup98 using lentivirus vector coexpressed H-2K^k, as described above, and at this time the culture was challenged with replication-competent EGFP-expressing HIV-1. Flow cytometric analysis indicated that numbers of HIV-1-infected cells were obviously inhibited in Nup98-siRNA-expressing T cells but not in control luciferase-specific siRNA-expressing cells. Significant reduction of HIV-1 p24^{gag} (five to sixfold) was also noted in the culture supernatant (data not shown). It was reported that Nup98 and Nup214 are required for Rev-dependent export of HIV-1 RNA [24]. Thus, inhibition of Nup98 expression by functional impairment of Nup98 by siRNA may induce inhibition of HIV-1 gene expression through inhibition of the Rev-dependent export. Some degree of the inhibitory effect of HIV-1 infection by the siRNA may be partly caused by this inhibitory effect of Rev function. But quantitative analysis of HIV-1 cDNA in single-round infection demonstrated that the inhibition of nuclear import of HIV-1 cDNA (Fig. 3G) was apart from gene expression. These findings suggest the involvement of a specific import pathway in the nuclear entry of HIV cDNA through NPC.

Most of the transport receptors identified to date are members of a large family of RanGTP binding proteins, which exhibit a limited sequence similarity to the Ran binding domain of importin β. The interaction of these receptors with Nups is regulated by small GTPase Ran. Ran is a small GTPase that cycles between a GDP-bound form (RanGDP) and a GTP-bound form (RanGTP) and plays an important role in both import and export [8]. The directional active nuclear transport is controlled by the different RanGDP and RanGTP concentration gradients within the cell. In the cytoplasm, a much higher concentration of RanGDP to RanGTP is maintained, and conversion of RanGDP to RanGTP occurs by exchanging the entire nucleotide and is catalyzed by the guanine nucleotide exchanging factor (RCC1) [33]. The exchange of the nucleotide and disassembly of importin β2 complex at a site on Nup98 was reported [13]. The VSV M-mediated inhibition of nuclear traffic is due to the inhibition of RanGDP to RanGTP conversion [13]. Therefore, in the presence of VSV M expression or inhibition of Nup98 expression should induce the disruption of the RanGDP and RanGTP concentration gradients. Our data strongly suggest

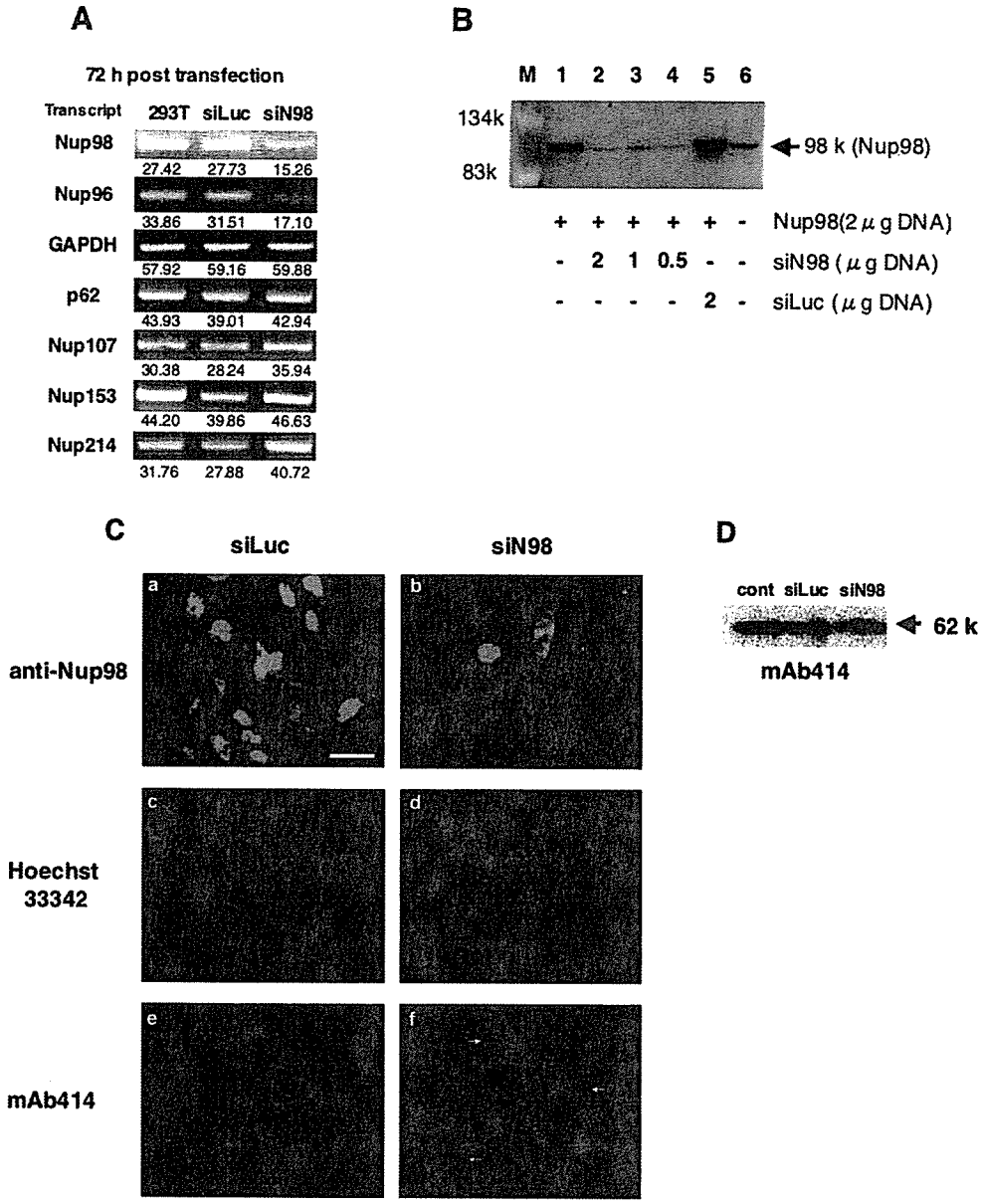

Fig. 3. Depletion of Nup98 by siRNA impairs specific NPC function. (A) Inhibition of Nup98 and Nup96 mRNA expression with Nup98-targeted siRNA. 293T cells were transfected with siRNA-expressing plasmid DNA targeted for Nup98 or luciferase (siN98 or siLuc, respectively) and mRNA levels of Nup98, Nup96, p62, Nup107, Nup153, Nup214 or GAPDH were determined by RT-PCR. The numbers under the band indicate intensity of each band digitalized by using NIH image. (B) Inhibition of Nup98 expression with siRNA-expressing plasmid DNA. Western blotting analysis using an anti-Nup98 antibody in siLuc or siN98-transfected 293T cells is indicated. Nup98-expressing plasmid (Nup98 as indicated) was transfected without (lane 1) or with (lane 2-5) siRNA-expressing plasmid as indicated. The expression level of endogenous Nup98 is indicated in lane 6. Size marker (M) is indicated. (C) Expression of Nup98 and localization of FG-repeat nucleoporins in siRNA-transduced cultures. Immunofluorescence analysis of HeLa cells infected with siLuc (a, c, e)- or siN98 (b, d, f)-expressing lentivirus vector using an anti-Nup98 (upper panels) or mAb414 antibody (lower panels) are shown. Hoechst 33342 staining (middle panels) indicates nucleus. Blue arrow in bottom panel indicates weak signal on nuclear rim, and white arrow indicates a shift labeling to the cytoplasm, probably annulate lamellae form. Calibration bar = 30 μm. (D) Western blotting analysis of HeLa cells infected with siRNA-expressing lentivirus vector using mAb414. The level of p62 protein expression is indicated. (E) Nuclear import assay of Nup98-depeleted HeLa cells. Cells were infected with the siLuc (upper panels)- or siN98 (lower panels)-expressing lentivirus vector, and 3 days later, nuclear import for these depleted cells after permealization with digitonin was examined using DsRed-labeled SV40 NLS (a, d), U1A (b, e), and rpL23a (c, f), respectively. Import of SV40 NLS is dependent on importin α/β and that of rpL23a is dependent on importin β3. Import of U1A is independent of active transfer machinery. The reaction was performed at 30 °C and stopped after 30 min by fixation. Calibration bar = 30 μm. Results of one representative assay from three independent experiments are shown (A, B, C, D, E). (F) Quantification of nuclear import. Cells with nuclear import were counted in five randomly selected visual fields. Data are expressed as percentage of imported cells (mean ± S.D. of five fields). *$P < 0.05$, compared with siLuc by Welch's t-test. (G) Measurement of newly synthesized HIV-1 cDNA in siLuc- or siN98-transfected cells. 293T cells were transfected with siN98- or siLuc-expressing plasmid DNA, and 72 h later, EGFP-expressing HIV-1 vector was used for infection. DNA was extracted 24 h after infection and DNA was subjected to real-time PCR assay. The number of HIV-1 cDNA copies per culture is indicated. A heat inactivated HIV-1 vector (HI) was used as negative control. Results are mean ± S.D. of six independent experiments. *$P < 0.05$, compared with siLuc by Welch's t-test.

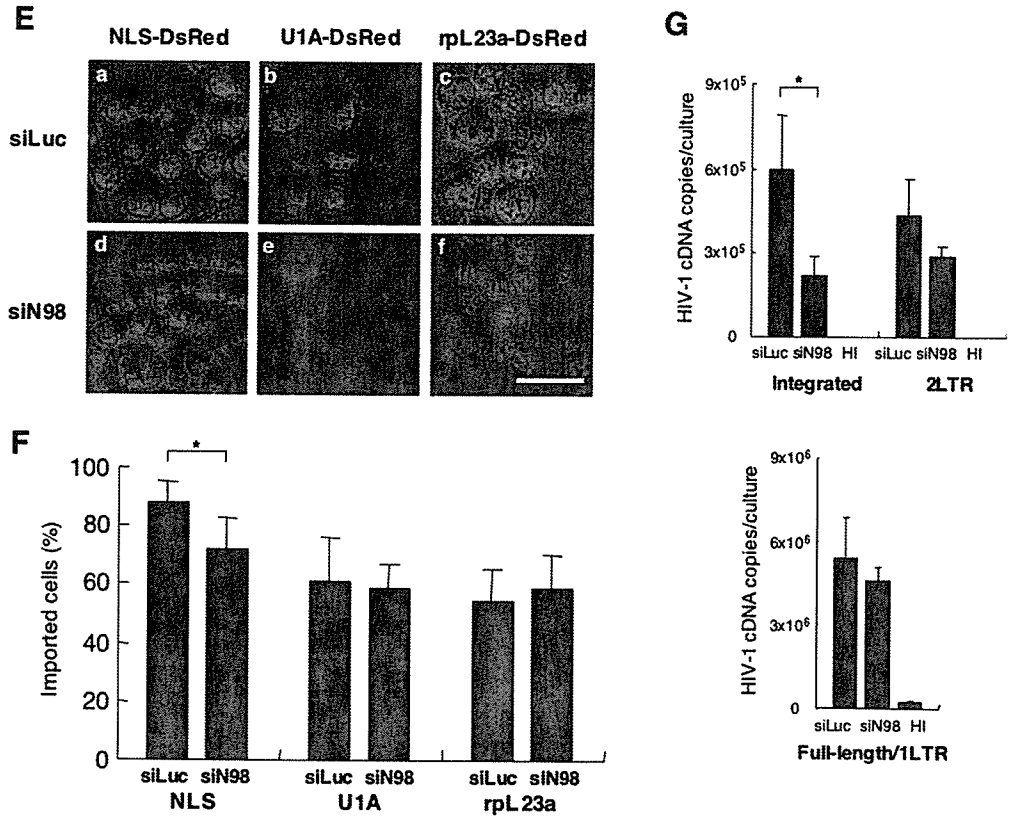

Fig. 3. *(continued)*

that these RanGTP/GDP gradients and localization of Nups are important for the directional active transport of HIV-1 cDNA. In fact, it has been recently reported that importin 7 is a major transport receptor for nuclear import of HIV-1 PIC [15]. Fassati et al. showed that PIC isolated from HIV-1-infected macrophages efficiently entered the nucleus mediated by importin 7 in a Ran- and energy-dependent manner.

Importin 7 is also known as a transport receptor for ribosomal proteins and histone H1 [28,34]. In our experiments, Nup98 depletion hampered the nuclear entry ability mediated by importin α/β, which was examined by NLS. In contrast, the nuclear entry abilities predominantly mediated by importin β3, which was examined by rpL23a, and these transporter-independent pathways, which were examined by U1A, were not affected in the Nup98-depleted NPC. Import of rpL23a was mediated alternatively by multiple transport receptors such as importin β, importin β2 (transportin), importin β3 and importin 7 [28]. It was reported that the mutant pore of Nup98-knockout cells has reduced affinity for many specific transport receptors, especially importin 7 [27]. Thus, it is possible that the functional association of importin 7 and Nup98 may disrupt and Nup98 depletion may induce impairment of the nuclear import pathway predominantly mediated by importin 7. In the present study, we did not succeed in establishing in vitro nuclear import assay of HIV-1 PIC using Nup98-depleted NPC. It will be very interesting to examine whether Nup98 is directly involved in the nuclear import of PIC. Further biochemical analyses, such as experiments showing large complex formation with PIC, importin 7, and Nup98 in infected cells are required.

In conclusion, we have demonstrated in the present study the role of Nup98 in the nuclear entry of HIV-1 cDNA in cultured cells. Our results suggest that a similar mechanism may be operative in HIV-1-infected individuals. Therefore, inhibition of Nup98 function could be a potentially important target for therapeutic intervention in patients with acquired immunodeficiency syndrome.

Acknowledgements

We thank Dr. H. Miyoshi, K. Taira and E. Izaurralde for providing several reagents used in our study. This work was supported by a Grant-in-Aid for Scientific Research on Priority Areas from the Ministry of Education, Culture, Sports, Science, and Technology of Japan; by grants for Research on HIV/AIDS and Health Sciences from the Ministry of Health, Labor and Welfare of Japan. Y. Koyanagi was also supported by the Naito Foundation.

References

[1] B.R. Cullen, Journey to the center of the cell, Cell 105 (2001) 697–700.

[2] J.B. Weinberg, T.J. Matthews, B.R. Cullen, M.H. Malim, Productive human immunodeficiency virus type 1 (HIV-1) infection of nonproliferating human monocytes, J. Exp. Med. 174 (1991) 1477–1482.

[3] M.I. Bukrinsky, N. Sharova, M.P. Dempsey, T.L. Stanwick, A.G. Bukrinskaya, S. Haggerty, M. Stevenson, Active nuclear import of human immunodeficiency virus type 1 preintegration complexes, Proc. Natl. Acad. Sci. USA 89 (1992) 6580–6584.

[4] L. Naldini, U. Blomer, P. Gallay, D. Ory, R. Mulligan, F.H. Gage, I.M. Verma, D. Trono, In vivo gene delivery and stable transduction of nondividing cells by a lentiviral vector, Science 272 (1996) 263–267.

[5] M.A. Rebolledo, P. Krogstad, F. Chen, K.M. Shannon, T.S. Klitzner, Infection of human fetal cardiac myocytes by a human immunodeficiency virus-1-derived vector, Circ. Res. 83 (1998) 738–742.

[6] H. Miyoshi, M. Takahashi, F.H. Gage, I.M. Verma, Stable and efficient gene transfer into the retina using an HIV-based lentiviral vector, Proc. Natl. Acad. Sci. USA 94 (1997) 10319–10323.

[7] W.C. Greene, B.M. Peterlin, Charting HIV's remarkable voyage through the cell: basic science as a passport to future therapy, Nat. Med. 8 (2002) 673–680.

[8] D. Gorlich, U. Kutay, Transport between the cell nucleus and the cytoplasm, Annu. Rev. Cell Dev. Biol. 15 (1999) 607–660.

[9] S. Nakielny, G. Dreyfuss, Transport of proteins and RNAs in and out of the nucleus, Cell 99 (1999) 677–690.

[10] M.P. Sherman, W.C. Greene, Slipping through the door: HIV entry into the nucleus, Microbes Infect. 4 (2002) 67–73.

[11] S.R. Wente, Gatekeepers of the nucleus, Science 288 (2000) 1374–1377.

[12] D. Stoffler, B. Fahrenkrog, U. Aebi, The nuclear pore complex: from molecular architecture to functional dynamics, Curr. Opin. Cell Biol. 11 (1999) 391–401.

[13] B.M. Fontoura, G. Blobel, N.R. Yaseen, The nucleoporin Nup98 is a site for GDP/GTP exchange on ran and termination of karyopherin beta 2-mediated nuclear import, J. Biol. Chem. 275 (2000) 31289–31296.

[14] I. Ben-Efraim, L. Gerace, Gradient of increasing affinity of importin beta for nucleoporins along the pathway of nuclear import, J. Cell Biol. 152 (2001) 411–417.

[15] A. Fassati, D. Gorlich, I. Harrison, L. Zaytseva, J.M. Mingot, Nuclear import of HIV-1 intracellular reverse transcription complexes is mediated by importin 7, EMBO J. 22 (2003) 3675–3685.

[16] S.L. Butler, M.S. Hansen, F.D. Bushman, A quantitative assay for HIV DNA integration in vivo, Nat. Med. 7 (2001) 631–634.

[17] Y. Suzuki, N. Misawa, C. Sato, H. Ebina, T. Masuda, N. Yamamoto, Y. Koyanagi, Quantitative analysis of human immunodeficiency virus type 1 DNA dynamics by real-time PCR: integration efficiency in stimulated and unstimulated peripheral blood mononuclear cells, Virus Genes 27 (2003) 177–188.

[18] M. Miyagishi, K. Taira, U6 promoter-driven siRNAs with four uridine 3′ overhangs efficiently suppress targeted gene expression in mammalian cells, Nat. Biotechnol. 20 (2002) 497–500.

[19] H. Miyoshi, K.A. Smith, D.E. Mosier, I.M. Verma, B.E. Torbett, Transduction of human CD34+ cells that mediate long-term engraftment of NOD/SCID mice by HIV vectors, Science 283 (1999) 682–686.

[20] C. von Kobbe, J.M. van Deursen, J.P. Rodrigues, D. Sitterlin, A. Bachi, X. Wu, M. Wilm, M. Carmo-Fonseca, E. Izaurralde, Vesicular stomatitis virus matrix protein inhibits host cell gene expression by targeting the nucleoporin Nup98, Mol. Cell 6 (2000) 1243–1252.

[21] V.W. Pollard, W.M. Michael, S. Nakielny, M.C. Siomi, F. Wang, G. Dreyfuss, A novel receptor-mediated nuclear protein import pathway, Cell 86 (1996) 985–994.

[22] P.F. Lewis, M. Emerman, Passage through mitosis is required for oncoretroviruses but not for the human immunodeficiency virus, J. Virol. 68 (1994) 510–516.

[23] C.E. Pritchard, M. Fornerod, L.H. Kasper, J.M. van Deursen, RAE1 is a shuttling mRNA export factor that binds to a GLEBS-like NUP98 motif at the nuclear pore complex through multiple domains, J. Cell Biol. 145 (1999) 237–254.

[24] A.S. Zolotukhin, B.K. Felber, Nucleoporins nup98 and nup214 participate in nuclear export of human immunodeficiency virus type 1 Rev, J. Virol. 73 (1999) 120–127.

[25] A. Bachi, I.C. Braun, J.P. Rodrigues, N. Pante, K. Ribbeck, C. von Kobbe, U. Kutay, M. Wilm, D. Gorlich, M. Carmo-Fonseca, E. Izaurralde, The C-terminal domain of TAP interacts with the nuclear pore complex and promotes export of specific CTE-bearing RNA substrates, RNA 6 (2000) 136–158.

[26] B.M. Fontoura, G. Blobel, M.J. Matunis, A conserved biogenesis pathway for nucleoporins: proteolytic processing of a 186-kilodalton precursor generates Nup98 and the novel nucleoporin, Nup96, J. Cell Biol. 144 (1999) 1097–1112.

[27] X. Wu, L.H. Kasper, R.T. Mantcheva, G.T. Mantchev, M.J. Springett, J.M. van Deursen, Disruption of the FG nucleoporin NUP98 causes selective changes in nuclear pore complex stoichiometry and function, Proc. Natl. Acad. Sci. USA 98 (2001) 3191–3196.

[28] S. Jakel, D. Gorlich, Importin beta, transportin, RanBP5 and RanBP7 mediate nuclear import of ribosomal proteins in mammalian cells, EMBO J. 17 (1998) 4491–4502.

[29] S.A. Adam, R.S. Marr, L. Gerace, Nuclear protein import in permeabilized mammalian cells requires soluble cytoplasmic factors, J. Cell Biol. 111 (1990) 807–816.

[30] G.R. Whittaker, Virus nuclear import, Adv. Drug Deliv. Rev. 55 (2003) 733–747.

[31] L.C. Trotman, N. Mosberger, M. Fornerod, R.P. Stidwill, U.F. Greber, Import of adenovirus DNA involves the nuclear pore complex receptor CAN/Nup214 and histone H1, Nat. Cell Biol. 3 (2001) 1092–1100.

[32] P.M. Ojala, B. Sodeik, M.W. Ebersold, U. Kutay, A. Helenius, Herpes simplex virus type 1 entry into host cells: reconstitution of capsid binding and uncoating at the nuclear pore complex in vitro, Mol. Cell Biol. 20 (2000) 4922–4931.

[33] J.Z. Gasiorowski, D.A. Dean, Mechanisms of nuclear transport and interventions, Adv. Drug Deliv. Rev. 55 (2003) 703–716.

[34] M. Bauerle, D. Doenecke, W. Albig, The requirement of H1 histones for a heterodimeric nuclear import receptor, J. Biol. Chem. 277 (2002) 32480–32489.

JOURNAL OF VIROLOGY, Aug. 2004, p. 8654–8662
0022-538X/04/$08.00+0 DOI: 10.1128/JVI.78.16.8654–8662.2004
Copyright © 2004, American Society for Microbiology. All Rights Reserved.
Vol. 78, No. 16

Spirodiketopiperazine-Based CCR5 Inhibitor Which Preserves CC-Chemokine/CCR5 Interactions and Exerts Potent Activity against R5 Human Immunodeficiency Virus Type 1 In Vitro

Kenji Maeda,[1,2] Hirotomo Nakata,[1,2] Yasuhiro Koh,[1,2] Toshikazu Miyakawa,[2] Hiromi Ogata,[1,2] Yoshikazu Takaoka,[3] Shiro Shibayama,[3] Kenji Sagawa,[3] Daikichi Fukushima,[3] Joseph Moravek,[4] Yoshio Koyanagi,[5] and Hiroaki Mitsuya[1,2,6]*

Department of Hematology[1] and Department of Infectious Diseases,[2] Kumamoto University School of Medicine, Kumamoto 860-8556, Minase Research Institute, Ono Pharmaceutical Co. Ltd., Osaka 618-8585,[3] and Department of Virology, Tohoku University Graduate School of Medicine, Sendai 980-8575,[5] Japan; Moravek Biochemicals, Inc., Brea, California 92821[4]; and Experimental Retrovirology Section, HIV and AIDS Malignancy Branch, National Cancer Institute, Bethesda, Maryland 20892[6]

Received 6 January 2004/Accepted 31 March 2004

We identified a novel spirodiketopiperazine (SDP) derivative, AK602/ONO4128/GW873140, which specifically blocked the binding of macrophage inflammatory protein 1α (MIP-1α) to CCR5 with a high affinity (K_d of ≈3 nM), potently blocked human immunodeficiency virus type 1 (HIV-1) gp120/CCR5 binding and exerted potent activity against a wide spectrum of laboratory and primary R5 HIV-1 isolates, including multidrug-resistant HIV-1 (HIV-1_{MDR}) (50% inhibitory concentration values of 0.1 to 0.6 nM) in vitro. AK602 competitively blocked the binding to CCR5 expressed on Chinese hamster ovary cells of two monoclonal antibodies, 45523, directed against multidomain epitopes of CCR5, and 45531, specific against the C-terminal half of the second extracellular loop (ECL2B) of CCR5. AK602, despite its much greater anti-HIV-1 activity than other previously published CCR5 inhibitors, including TAK-779 and SCH-C, preserved RANTES (regulated on activation normal T-cell expressed and secreted) and MIP-1β binding to $CCR5^+$ cells and their functions, including CC-chemokine-induced chemotaxis and CCR5 internalization, while TAK-779 and SCH-C fully blocked the CC-chemokine/CCR5 interactions. Pharmacokinetic studies revealed favorable oral bioavailability in rodents. These data warrant further development of AK602 as a potential therapeutic for HIV-1 infection.

Highly active antiretroviral therapy has had a major impact on the AIDS epidemic in industrially advanced nations (5, 20); however, eradication of human immunodeficiency virus type 1 (HIV 1) appears to be currently impossible, in part due to the viral reservoirs remaining in blood and infected tissues (6, 27). The limitation of antiviral therapy of AIDS is exacerbated by complicated regimens, the development of drug-resistant HIV-1 variants (11), and a number of inherent adverse effects. Successful antiviral drugs, in theory, exert their virus-specific effects by interacting with viral receptors, virally encoded enzymes, viral structural components, viral genes, or their transcripts without disturbing cellular metabolism or function (20). However, at present, no antiretroviral drugs or agents are likely to be completely specific for HIV-1 or to be devoid of toxicity or side effects in the therapy of AIDS, which has been a critical issue because patients with AIDS and its related diseases will have to receive antiretroviral therapy for a long period of time, perhaps for the rest of their lives (6, 27). Thus, the identification of new antiretroviral drugs which have unique mechanisms of action and produce no or minimal side effects remains an important therapeutic objective (20). In this respect, it has been thought that certain chemokine receptor inhibitors might produce no or minimal toxicity.

In the present study, we designed, synthesized, and identified a novel small nonpeptidic CCR5 inhibitor, AK602/ONO4128/GW873140, and related compounds which showed high binding affinity to CCR5, potently inhibited CCR5 gp120 interactions, and had potent HIV-1-specific antiviral activity against laboratory and clinical strains of HIV-1, including highly drug-resistant HIV-1 variants. We describe here the pharmacological characteristics of AK602/ONO4128/GW873140 and its unique feature that, despite the compound's much greater anti-HIV-1 activity compared to previously published CCR5 inhibitors, AK602/ONO4128/GW873140 preserves RANTES and MIP-1β binding to $CCR5^+$ cells and their functions.

MATERIALS AND METHODS

Reagents. Two newly designed and synthesized spirodiketopiperazine (SDP) derivatives, AK530 [(3*S*)-1-but-2-yn-1-yl-3-[(1*S*)-cyclohexylhydroxymethyl]-9 (3,5-dimethyl-1-phenyl-1H-pyrazol-4-ylmethyl)-1,4,9-triazaspiro[5.5]undecane 2,5-dione dihydrochloride] and AK602 [4-[4-[(3*R*)-1-butyl-3-[(1*R*) cyclohexylhydroxymethyl]-2,5-dioxo-1,4,9-triazaspiro[5.5]undec-9-yl methyl]phenoxy]benzoic acid hydrochloride], are discussed in the present report. The methods for their synthesis and physicochemical profiles will be described elsewhere. The structures of these two compounds are shown in Fig. 1. A previously reported prototypic SDP derivative, E913 (17), was used as a reference compound. E921 and

* Corresponding author. Mailing address: Department of Hematology, Kumamoto University School of Medicine, 1-1-1 Honjo, Kumamoto 860-8556, Japan. Phone: 81-96-373-5156. Fax: 81-96-363-5265. E-mail: hmitsuya@helix.nih.gov.

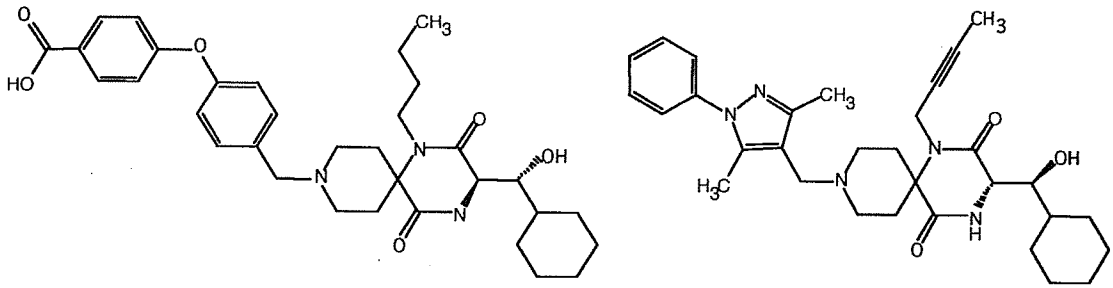

AK602 Mr. 614.2 AK530 Mr. 604.6

FIG. 1. Structures of AK602 and AK530.

AK671, which have the same structures as CCR5 inhibitors TAK-779 and SCH-351125 (SCH-C), respectively, were synthesized as previously described by others (1, 28).

Zidovudine was purchased from Sigma (St. Louis, Mo.). Nelfinavir and saquinavir were provided by Japan Energy (Tokyo, Japan) and Roche Products (Welwyn Garden City, United Kingdom), respectively.

^{125}I-labeled chemokines macrophage inflammatory protein-1α (MIP-1α), macrophage inflammatory protein-1β (MIP-1β), and RANTES were purchased from Amersham Pharmacia Biotech (Little Chalfont, United Kingdom) and PerkinElmer Life Sciences, Inc. (Boston, Mass.), and three corresponding unlabeled chemokines (MIP-1α, MIP-1β, and RANTES) were purchased from PeproTech Inc. (Rocky Hill, N.J.). Recombinant HIV-1_{YU2} gp120 (rgp120) and human soluble CD4 (sCD4) were purchased from Immuno Diagnostics, Inc. (Woburn, Mass.).

Cells, viruses, and anti-HIV-1 assay. Chinese hamster ovary (CHO) cells expressing CCR5 (17) were maintained in Ham's F-12 medium (Gibco-BRL, Rockville, Md.) supplemented with 10% fetal calf serum (JRH Biosciences, Lenaxa, Kans.), 50 U of penicillin per ml, and 50 μg of streptomycin per ml in the presence of 5 μg of blasticidin S hydrochloride per ml. Peripheral blood mononuclear cells were isolated from buffy coats of HIV-1-seronegative individuals with Ficoll-Hypaque density gradient centrifugation and cultured at a concentration of 10^6 cells/ml in RPMI 1640-based culture medium supplemented with 10% fetal calf serum and antibiotics with 10 μg of phytohemagglutinin per ml for 3 days prior to use (phytohemagglutinin-peripheral blood mononuclear cells). Cell line CCR5$^+$ MOLT4 (18) was a kind gift from Yosuke Maeda, Kumamoto University, Japan.

A panel of HIV-1 strains was employed for drug susceptibility assays: HIV $1_{Ba\text{-}L}$ (8), HIV-$1_{JR\text{-}FL}$ (13) HIV-$1_{NL4\text{-}3}$ (34), a wild-type HIV-1_{MOKW} isolated from a drug-naive AIDS patient (17), and two multidrug-resistant (HIV-1_{MDR}) primary HIV-1 strains (HIV-1_{JSI} and HIV-1_{MM}) (36). All primary HIV-1 strains were passaged once or twice in phytohemagglutinin-peripheral blood mononuclear cell cultures, and the culture supernatants were stored at −80°C until use. Antiviral assays with phytohemagglutinin-peripheral blood mononuclear cells were conducted as previously reported (12, 17, 26).

HIV-1 gp120 binding inhibition assays. CCR5$^+$ CHO cells were incubated with rgp120 (5 μg/ml) and sCD4 at 5 μg/ml, biotinylated with EZ-link sulfo-NHS-SS-biotin (Pierce, Rockford, Ill.) in the presence of the indicated concentrations of a CCR5 inhibitor for 1 h at 37°C. Cells were washed, and the binding of the rgp120-sCD4 complex to CCR5$^+$ CHO cells was determined with phycoerythrin-conjugated streptavidin (BD PharMingen, San Diego, Calif.). Nonspecific binding was determined based on the mean florescence intensity of phycoerythrin-conjugated streptavidin with sCD4 but without rgp120. Drug concentrations that brought about 50% inhibition (IC_{50}) of mean fluorescence intensity were then determined.

Generation of ^{3}H-labeled CCR5 inhibitors. Five CCR5 inhibitors, AK530, AK602, E913, E921/TAK-779, and AK671/SCH-C, were tritiated by reductive amination with sodium triacetoxyborotritide (10), methylation with [^{3}H]methyliodide, and heterogeneous catalytic exchange with tritium gas (4). Detailed description of the radiosynthesis of the inhibitors will be presented by J.M. elsewhere. In brief, [^{3}H]E913, [^{3}H]AK530, and [^{3}H]AK602 were prepared by reductive amination of the corresponding aldehyde with piperidine-containing components of each inhibitor with an excess of sodium triacetoxyborotritide, and the tritium label was positioned selectively into the methylene group connecting the two components, generating inhibitors with specific activities of 10.2 Ci/mmol, 17.5 Ci/mmol, and 8.3 Ci/mmol, respectively. [^{3}H]E921/TAK-779 was prepared by methylating the *N*-methyl precursor of E921/TAK-779 with [^{3}H]methyliodide, generating [^{3}H]E921/TAK-779, with a specific activity of 6.1 Ci/mmol. For the preparation of [^{3}H]AK671/SCH-C, methyl-2,4-dimethylpyridine-3-carboxylate was tritiated by an exchange with tritium gas, catalyzed by palladium on carbon in ethanol and triethylamine. Its conversion to N-oxide and alkaline hydrolysis of the resulting ester provided [^{3}H]2,4-dimethyl-pyridine-3-carboxylic acid. Its condensation with *N-tert*-butoxycarbonyl precursor provided [^{3}H]AK671/SCH-C, with a specific activity of 5 Ci/mmol.

Saturation binding assay. CCR5$^+$ CHO cells (1.5×10^5 cells/well) were plated onto 48-well, flat-bottomed culture plates, incubated for 24 h, rinsed with Ham's F-12 medium containing 20 mM HEPES and 0.5% bovine serum albumin (Sigma), exposed to various concentrations of each ^{3}H-labeled CCR5 inhibitor, washed thoroughly with cold phosphate-buffered saline, and lysed with 0.5 ml of 1 N NaOH, and the radioactivity in the lysates was measured. The nonspecific binding of a radiolabeled compound was determined based on the radioactivity detected in the CCR5$^+$ CHO cell-plated wells containing the same amount of the ^{3}H-labled CCR5 inhibitor and a 200-fold greater amount of the corresponding non radiolabeled compound. The K_d (dissociation) values of CCR5 inhibitors and the maximal binding values (B_{max} = number of CCR5/cell) were calculated based on their specific radioactivity with Graphpad Prism software (Intuitive Software for Science, San Diego, Calif.). All assays were performed in duplicate, and the values shown in this report are the arithmetic means (±1 standard deviation) of 3 to 10 independently conducted assays.

Chemokine binding inhibition and chemotaxis inhibition assays. CCR5$^+$ CHO cells (1.5×10^5) were plated onto 48-well microculture plates, incubated for 24 h, rinsed, exposed to 3 nM [^{125}I]MIP-1α, [^{125}I]MIP-1β, or [^{125}I]RANTES in the presence of various concentrations of a CCR5 inhibitor at room temperature for 1 h, thoroughly washed with phosphate-buffered saline, and lysed with 0.5 ml of 1 N NaOH, and their radioactivity was counted. The nonspecific binding of the labeled chemokine to the cells was determined based on the radioactivity detected in the wells plated with the same number of CCR5-negative CHO (CHO-K1) cells exposed to each radiolabeled chemokine (3 nM).

Chemotaxis inhibition assays were conducted with CCR5$^+$ MOLT4 cells and the ChemTx System (Neuro Probe, Inc., Gaithersburg, Md.). In brief, CCR5$^+$ MOLT4 cells were exposed to various concentrations of each CCR5 inhibitor for 30 min, thoroughly rinsed, plated onto the upper chamber of the ChemTx System, exposed to 0.5 nM RANTES contained in the lower chamber, and incubated for 4 h at 37°C, and the number of the cells which migrated from the upper chamber to the lower chamber was determined. Percent chemotaxis was determined with the formula 100 × [(number of CCR5 inhibitor-exposed cells which migrated to the lower chamber in the presence of RANTES) − (number of CCR5 inhibitor-unexposed cells which migrated to the lower chamber in the absence of RANTES)]/[(number of CCR5 inhibitor-unexposed cells which migrated to the lower chamber in the presence of RANTES) − (number of CCR5 inhibitor-unexposed cells which migrated to the lower chamber in the absence of RANTES)].

FACS analysis. Fluorescence-activated cell sorting (FACS) analysis was performed as previously described (17) with minor modifications. Briefly, CCR5$^+$ CHO cells (3×10^5) were stained with a phycoerythrin- or fluorescein isothiocyanate-conjugated anti-CCR5 monoclonal antibody 2D7 (BD PharMingen, San Diego, Calif.) or 45523 or 45531 (R&D Systems, Minneapolis, Minn.), with or without a test CCR5 inhibitor, washed, and examined with an Epics XL (Beckman Coulter, Fullerton, Calif.).

RESULTS

Potent activity of AK602 against R5 wild-type and multidrug-resistant R5 HIV-1. We have previously reported that a prototypic SDP derivative, E913, was active against R5 HIV-1 in vitro, with IC_{50} values of 30 to 60 nM as tested in target phytohemagglutinin-treated peripheral blood mononuclear cells (17). Following optimization for increased potency against R5 HIV-1 and favorable pharmacokinetic features, we identified AK602 as the most potent agent among newly designed and synthesized SDP derivatives. AK602 exerted potent activity against three wild-type R5 HIV-1 strains (HIV-$1_{Ba\text{-}L}$, HIV $1_{JR\text{-}FL}$ and HIV-1_{MOKW}) with IC_{50} values of 0.1 to 0.4 nM (Table 1). It was of note that AK602 was substantially more potent than two previously published CCR5 inhibitors, E921/TAK-779 and AK671/SCH-C (1, 28).

During the extended study of the antiviral activity of the prototypic E913, we noted that its activity against R5 HIV-$1_{Ba\text{-}L}$ in vitro varied substantially; the range of IC_{50} values spanned from 14 to 650 nM (Fig. 2). When we tested the activity of E921/TAK-779 in phytohemagglutinin-treated peripheral blood mononuclear cells from multiple seronegative donors, its variability was also substantial: its IC_{50} values varied from 2 to 200 nM. However, when we tested AK602, the variability of AK602's anti-HIV-1 activity was limited and similar to that seen for zidovudine. The difference in the range of the CCR5 inhibitor's IC_{50} values seems to correlate with the potency of the inhibitor examined. Indeed, we have seen a greater variability in the antiviral activity of the prototypic E913 (Fig. 2). Moreover, AK602 suppressed the infectivity and replication of two HIV-1_{MDR} variants, HIV-1_{MM} and HIV-1_{JSL} (36), at extremely low concentrations (IC_{50} values of 0.4 to 0.6 nM), while these two R5 HIV-1 variants were less susceptible to zidovudine, nelfinavir, and saquinavir (IC_{50} values were greater by factors of 10 to 36, >83, and 27 to 32, respectively, compared to those against HIV-$1_{Ba\text{-}L}$). As expected, none of these CCR5 inhibitors suppressed the infectivity and replication of X4 HIV-$1_{NL4\text{-}3}$ in vitro. Although certain CC-chemokines reportedly enhance the replication of X4 HIV-1 (19, 22), no such enhancement of X4 HIV-1 replication was seen with the CCR5 inhibitors examined in this study at concentrations of up to 1 μM (data not shown).

CCR5 binding properties of SDP derivatives. We determined the CCR5 binding profiles of SDP derivatives and compared them with those of previously published CCR5 inhibitors in saturation binding assays employing ^{3}H-labeled compounds. Figure 3A depicts the CCR5 binding profile of AK602, showing that it binds with high affinity to CCR5. The K_d values thus determined for AK602, E913, E921/TAK-779, and AK671/SCH-C were 2.9 ± 1.0 (Fig. 3A), 111.7 ± 3.5, 32.2 ± 9.6, and 16.0 ± 1.5 nM (data not shown), respectively.

We also asked whether the SDP derivatives blocked the binding to CCR5 of rgp120 following exposure to sCD4. As shown in Fig. 3B, AK602 potently blocked rgp120/sCD4 binding to CCR5 with an IC_{50} value of 2.7 nM, followed by E921/TAK-779 and AK-671/SCH-C, with IC_{50} values of 12.0 and 16.5 nM, respectively. When we asked whether AK602 blocked the intracellular Ca^{2+} mobilization induced by MIP-1α, MDC, SDF-1α, and MCP-1, whose primary receptors are CCR5, CCR4, CXCR4, and CCR2, respectively, with the method we

TABLE 1. Anti-HIV-1 activity of SDP derivatives

Compound	Mean IC_{50} (IC_{90}) ± SD in p24 assay (nM)						CC_{50}[a] (μM)
	HIV-$1_{Ba\text{-}L}$ (R5)	HIV-$1_{JR\text{-}FL}$ (R5)	HIV-1_{MOKW}[b] (R5)	HIV-1_{MM}[b] ($R5_{MDR}$)	HIV-1_{JSL}[b] ($R5_{MDR}$)	HIV-$1_{NL4\text{-}3}$ (X4)	
AK602	0.4 ± 0.3 (12 ± 10)	0.1 ± 0.1 (4 ± 2)	0.2 ± 0.1 (5 ± 3)	0.6 ± 0.2 (11 ± 2)	0.4 ± 0.3 (7 ± 2)	>1,000	50
AK530	32 ± 27 (324 ± 120)	13 ± 4 (144 ± 60)	ND[c]	ND	ND	>1,000	60
E913	82 ± 58 (709 ± 256)	81 ± 46 (>1,000)	51 ± 14 (941 ± 201)	61 ± 28 (>1,000)	64 ± 30 (713 ± 405)	>1,000	50
E921/TAK-779	28 ± 32 (256 ± 169)	5 ± 1 (237 ± 25)	11 ± 7 (194 ± 168)	14 ± 8 (352 ± 180)	7 ± 4 (316 ± 151)	>1,000	50
AK671/SCH-C	4 ± 2 (79 ± 52)	2 ± 0.5 (56 ± 57)	2 ± 1 (54 ± 20)	3 ± 0.5 (138 ± 25)	2 ± 0.3 (84 ± 18)	>1,000	>100
Zidovudine	7 ± 4 (48 ± 21)	10 ± 9 (157 ± 72)	6 ± 5 (47 ± 20)	250 ± 98 (>1,000)	70 ± 64 (>1,000)	11 ± 5 (181 ± 90)	>100
Nelfinavir	12 ± 8 (105 ± 48)	ND	14 ± 8 (82 ± 56)	>1,000	>1,000	20 ± 7 (75 ± 52)	ND
Saquinavir	11 ± 5 (60 ± 21)	ND	5 ± 2 (49 ± 40)	300 ± 65 (>1,000)	350 ± 105 (>1,000)	10 ± 4 (48 ± 2)	ND

[a] Cytotoxic concentrations of a compound that reduces the number of cells by 50% (CC_{50}) were determined as previously reported (17).
[b] HIV-1_{MOKW} was isolated from a drug-naive AIDS patient (17), while HIV-1_{MM} and HIV-1_{JSL} were from patients who received antiretroviral therapy for a long period and whose virus acquired a number of mutations in the RT- and PR-encoding HIV-1 genes (36).
[c] ND, not determined.

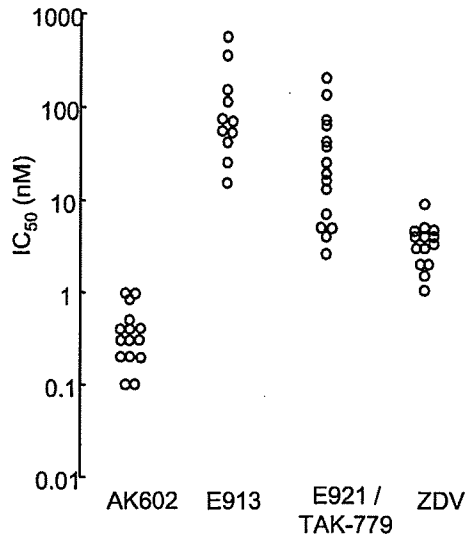

FIG. 2. Variability of anti-HIV-1 activity of AK602 in phytohemagglutinin-peripheral blood mononuclear cells. The range of IC_{50} values of E913 and E921/TAK-779 against HIV-1_{Ba-L} varied substantially when examined in multiple phytohemagglutinin-peripheral blood mononuclear cells as target cells, 14 to 650 nM (n = 11) and 2 to 200 nM (n = 15), respectively, while that of AK602 was relatively narrow, 0.1 to 1 nM (n = 15), similar to that of zidovudine (ZDV), 1 to 9 nM (n = 14).

published previously (17), AK602 completely blocked MIP-1α-induced Ca^{2+} mobilization at 0.1 μM and beyond; however, it failed to block Ca^{2+} mobilization induced with MDC, SDF-1α, and MCP-1 (data not shown).

We also attempted to illustrate where AK602 binds on the CCR5 molecule by employing several monoclonal antibodies known to bind to different domains of CCR5. FACS analyses revealed that there was no AK602 inhibition of the binding of monoclonal antibody 2D7, known to bind to the N-terminal half (or domain A) of the second extracellular loop of CCR5 (14) (Fig. 4). In contrast, AK602 competitively blocked the binding of two different monoclonal antibodies, 45523, reportedly directed against multidomain epitopes of CCR5, and 45531, which is known to be specific against the C-terminal half (or domain B) of the second extracellular loop (ECL2B) of CCR5 (14), as examined with $CCR5^+$ CHO cells (Fig. 4). These data suggest that the potent activity of AK602 against R5 HIV-1 stems from its binding to ECL2B and/or its vicinity with high affinity, resulting in inhibition of gp120/CD4 binding to CCR5. It was of note, however, that another SDP derivative, AK530, whose antiviral activity was moderate (the IC_{50} value against HIV-1_{Ba-L} was 32 nM; Table 1), whose rgp120/sCD4 binding inhibition was the lowest among the inhibitors examined (IC_{50}, 280 nM; Fig. 3B), and had only a moderate effect on the binding of monoclonal antibody 45531 to $CCR5^+$ cells (data not shown), had the highest binding affinity to CCR5 (K_d value, 0.4 nM; data not shown) among the SDP derivatives, suggesting that the binding pocket (or subsite) of certain SDP derivatives (such as AK530) does not quite overlap that of AK602.

SDP derivatives bind to CCR5 but permit RANTES and MIP-1β to bind to CCR5. We asked whether SDP derivatives blocked the binding of CC-chemokines to CCR5 expressed on the surface of CHO cells with [^{125}I]RANTES, [^{125}I]MIP-1α, and [^{125}I]MIP-1β and CCR5 inhibitors AK602, AK530, E921/TAK-779, and AK671/SCH-C. As shown in Fig. 5A, the concentrations of E921/TAK-779 and AK671/SCH-C which

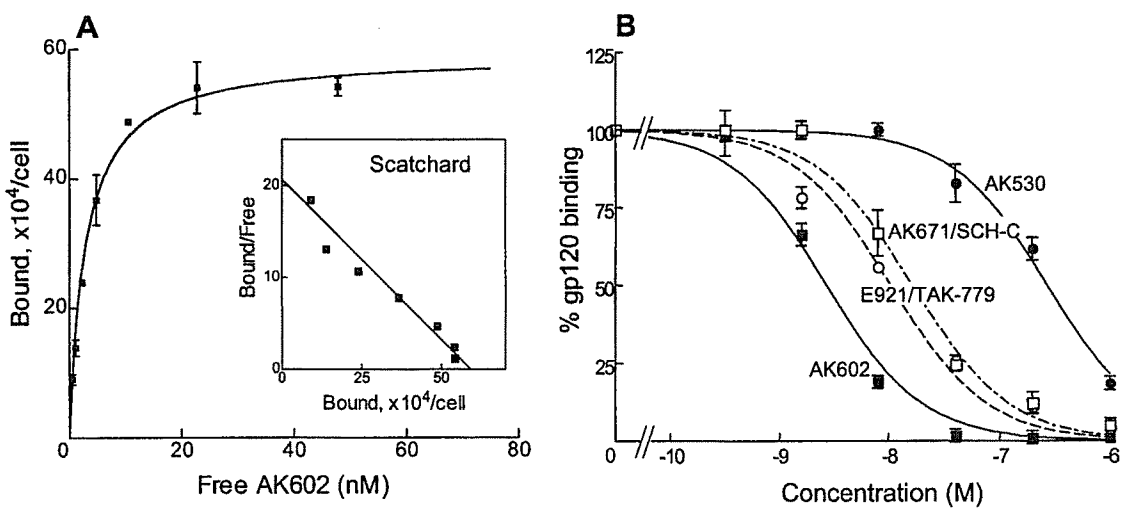

FIG. 3. CCR5 binding profiles and rgp120 binding blocking of various CCR5 inhibitors. (A) Binding affinity of AK602 to CCR5. $CCR5^+$ CHO cells were incubated with the ^{3}H-labeled CCR5 inhibitors AK530, AK602, E913, E921/TAK-779, and AK671/SCH-C for 1 h. Following thorough washing, cells were lysed, the radioactivity in the lysates was determined, and B_{max} and K_d values were calculated. The K_d values thus obtained were 0.4 ± 0.4, 2.9 ± 1.0, 111.7 ± 3.5, 32.2 ± 9.6, and 16.0 ± 1.5 nM, respectively. All assays were independently performed 3 to 10 times, and the values represent the arithmetic means ± 1 standard deviation. (B) AK602 potently blocks the binding of rgp120/sCD4 to CCR5. $CCR5^+$ CHO cells were incubated with rgp120 (5 μg/ml) and sCD4 (5 μg/ml) in the presence or absence of the indicated concentrations of CCR5 inhibitors, and the binding of rgp120/sCD4 complex to $CCR5^+$ CHO cells was determined. The 50% binding inhibition (EC_{50}) value was determined based on the mean fluorescence intensity values obtained with or without CCR5 inhibitors. EC_{50} values for AK602, AK530, E921/TAK-779, and AK671/SCH-C were 2.7, 280, 12.0, and 16.5 nM, respectively.

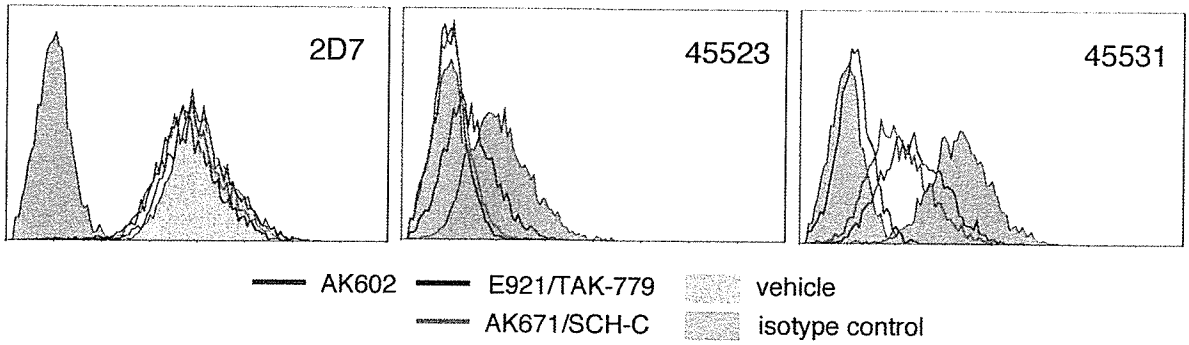

FIG. 4. AK602 binds to the second extracellular loop of CCR5. AK602 at 100 nM almost completely inhibited the binding of two monoclonal antibodies, 45523, directed against multidomain epitopes of CCR5, and 45531, recognizing ECL2B of CCR5. In contrast, E921/TAK-779 and AK671/SCH-C moderately blocked the binding of 45523 and 45531. Note that there was no AK602 inhibition of the binding of a monoclonal antibody 2D7, which is known to bind to domain A of ECL2 of CCR5.

blocked RANTES binding to CCR5 by 50% (IC_{50}) were 110 and 40 nM, respectively, and RANTES binding was completely blocked in the presence of ≥10 μM E921/TAK-779 or AK671/SCH-C. In contrast, AK602 only partially blocked RANTES binding to CCR5 by 40% even at 10 μM (Fig. 5A). The binding of MIP-1β to CCR5 was also completely blocked by E921/TAK-779 and AK671/SCH-C; however, AK602 failed to completely block MIP-1β binding (Fig. 5B). The MIP-1β binding value in the presence of 10 μM AK602 was 10%, and no further blockade occurred at higher concentrations up to 40 μM (data not shown). AK530 also failed to completely block the binding of RANTES and MIP-1β to CCR5.

These data suggest that the binding pockets (or subsites) of CCR5 for SDP derivatives only partially overlap the CC-chemokine binding sites of CCR5 or that the conformational changes ensuing the binding of SDP derivatives to CCR5 have only moderate effects on the binding of RANTES and MIP-1β. In the initial search for CCR5 inhibitors, lead compounds were sought as those inhibiting MIP-1α binding to CCR5 and MIP-1α-driven cytosolic Ca^{2+} flux, and thus, as expected, AK602 blocked MIP-1α binding to CCR5 although AK530 was substantially less potent in blocking MIP-1α binding (Fig. 5C). E921/TAK-779 and AK671/SCH-C were also found to completely block MIP-1α binding to CCR5 (Fig. 5C).

AK602 and RANTES bind simultaneously to CCR5. As described above, AK602 and AK530 only partially inhibited RANTES binding to $CCR5^+$ CHO cells; however, it was not clear whether those SDP derivatives and RANTES bound simultaneously to CCR5. Therefore, competitive binding assays employing ^3H-labeled and unlabeled AK602 and ^{125}I-labeled and unlabeled RANTES were conducted. As shown in Fig. 6A, the binding of [^3H]AK602 (10 nM) to CCR5 was only partially inhibited by ≥4 nM RANTES. Also, the binding of [^{125}I]RANTES at 8 nM was only inhibited by up to 20% in the presence of 10 nM AK602 (Fig. 6B).

The interpretation that AK602 and RANTES bind simultaneously to CCR5 was corroborated by another experiment in which a lower concentration of [^3H]AK602 and much higher concentrations of RANTES were used (Fig. 6A, inset). The radioactivity counted for [^3H]AK602 (5 nM) bound to $CCR5^+$ CHO cells was only moderately blocked in the presence of 100 and 1,000 nM RANTES, by 32 and 46%, respectively (Fig. 6A, inset). These data suggest that the SDP derivatives, in particular AK602, and RANTES bind simultaneously to CCR5, al-

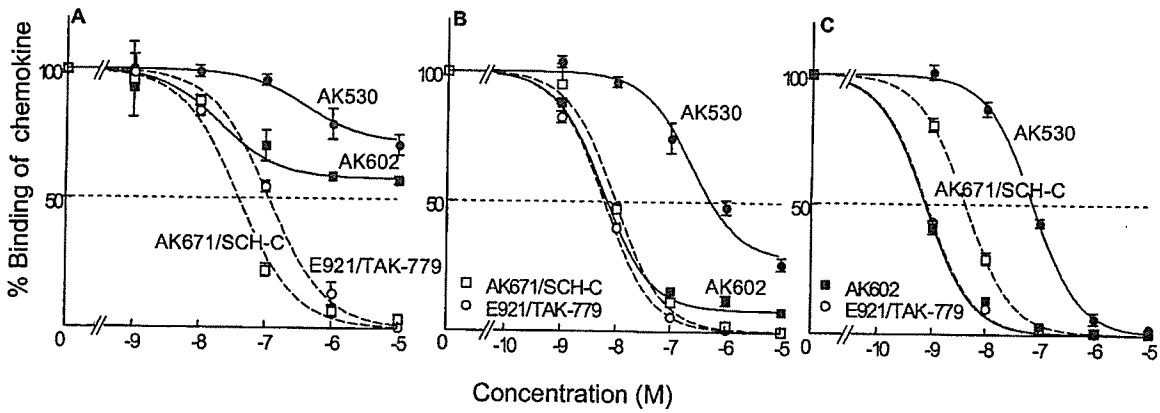

FIG. 5. Inhibition of CC-chemokine binding to CCR5 by various CCR5 inhibitors. $CCR5^+$ CHO cells were incubated with 3 nM [^{125}I]RANTES (A), [^{125}I]MIP 1 β (B), or [^{125}I]MIP-1 α (Pnel C) in the presence and absence of various concentrations of CCR5 inhibitors. Note that while AK671/SCH-C and E921/TAK-779 completely inhibited the binding of [^{125}I]RANTES, [^{125}I]MIP-1α, and [^{125}I]MIP-1β to CCR5, SDP derivatives partially blocked RANTES (A) and MIP-1β (B) binding, although they completely blocked MIP-1α binding (C).